To the Graduate Council:

I am submitting herewith a thesis written by William Pryor Gilchrist entitled "Theoretical Cross-Polarization Response of a Phased Array Antenna Composed of Circularly Polarized Ferrite Phase Shifters". I have examined the final copy of this thesis for form and content and recommend that it be accepted in partial fulfillment of the requirements for the degree of Master of Science, with a major in Engineering Science and Mechanics.

John E. Caruthers

John E. Caruthers, Major Professor

We have read this thesis
and recommend its acceptance:

Accepted for the Council:

Associate Vice Chancellor
and Dean of the Graduate School

STATEMENT OF PERMISSION TO USE

In presenting this thesis in partial fulfillment of the requirements for a Master's degree at the University of Tennessee, Knoxville, I agree that the Library shall make it available to borrowers under rules of the library. Brief quotations from this thesis are allowable without special permission, provided that accurate acknowledgment of the source is made.

Permission for extensive quotation from of reproduction of this thesis may be granted by my major professor, or in his absence, by the Head of Interlibrary Services when, in the opinion of either, the proposed use of the material is for a scholarly purpose. Any copying or use of the material in this thesis for financial gain shall not be allowed without my written permission.

Signature ______________

Date 25 May 1994

Theoretical Cross-Polarization Response of a Phased Array Antenna Composed of Circularly Polarized Ferrite Phase Shifters

A Thesis

Presented for the

Master of Science Degree

The University of Tennessee, Knoxville

William Pryor Gilchrist

August 1994

ACKNOWLEDGMENTS

The author would like to express his sincere appreciation to his family who has always provided support and encouragement in his pursuits.

He would also like to acknowledge the help and cooperation of his major professor, Dr. John Caruthers.

ABSTRACT

The purpose of this research is to show how a phased array antenna's susceptibility to cross-polarization jamming is directly correlated with the polarization characteristics of the individual phase shifters. The antenna under consideration is a space fed phased array antenna utilizing circularly polarized Faraday rotator type ferrite phase shifters. It is found that phased array antennas composed of phase shifters whose cross-polarization response slope is approximately -1, are most robust in their immunity to cross-polarization jamming.

TABLE OF CONTENTS

LIST OF FIGURES

NOMENCLATURE

n	Element number in the horizontal direction
m	Element number in the vertical direction
N	Number of elements in the horizontal direction
M	Number of elements in the vertical direction
θ_s	Denotes antenna scan angle relative to boresight
ϕ_s	Denotes antenna scan angle relative to the x-axis
d_x	Element spacing in the vertical direction
d_y	Element spacing in the horizontal direction
λ	Wavelength
a	Aperture width
$A(x)$	One dimensional continuous illumination function
$A(n)$	One dimensional discrete illumination function
$A(n,m)$	Two dimensional discrete illumination function
a_0	The magnitude of the uniform component of the illumination function
a_1	The magnitude of the cosine squared component of the illumination function
f	Distance from the feed horn to the array face
r_n	Distance from the n^{th} element to the center of the array
r_m	Distance from the m^{th} element to the center of the array

$E(\theta)$	One dimensional antenna radiation pattern
$E(\theta,\phi)$	Two dimensional antenna radiation pattern
$SENS$	Monopulse ratio including cross-polarization effects
REF	Monopulse ratio excluding cross-polarization effects
l	Phase shifter length
$\Gamma_{\pm}$	Propagation constant
$\alpha_{\pm}$	Attenuation constant
$\beta_{\pm}$	Phase constant
β_0	Dielectric constant
S_l	Waveguide cross-sectional area
ΔS_l	Ferrite cross-sectional area
χ_e^{eff}	Effective susceptibility
$\chi'_{\pm}$	Dispersive part of susceptibility
$\chi''_{\pm}$	Dissipative part of susceptibility
σ_o	Co-polarization radar cross-section
σ_c	Cross-polarization radar cross-section
E_{OD}	Co-polarization difference E field
E_{OS}	Co-polarization sum E field
E_{CD}	Cross-polarization difference E field
E_{CS}	Cross-polarization sum E field
J	Cross-polarization power

S	Co-polarization power
δ	Relative measure of susceptibility
N_{pe}	Number of points assessed to be vulnerable
N_{pt}	Number of points tested

CHAPTER I

INTRODUCTION

A. INTRODUCTORY REMARKS

In the development of modern radar systems, the antenna represents a crucial and costly design element. Phased array antennas, although typically the most costly, provide the flexibility required by many modern radar systems. The usefulness of a phased array antenna system is probably most apparent, and thus most exploited in defense related applications.

Figure 1.1 depicts the various functions of the phased array antenna as utilized by the U.S. Army's PATRIOT missile system. The electronically steered phased array antenna beam provides the radar system multi-function capability to track several targets simultaneously, perform large volume searches, illuminate targets for semi-active seekers, as well as serve as a communications link.[1,2]

In this paper, the author presents a mathematical model of a phased array antenna. The antenna under consideration is a space feed array utilizing circularly polarized Faraday rotator type ferrite phase shifters. Associated with the antenna are polarization characteristics inherent from the choice of ferrite used to make the phase shifters.

From this analysis, we will gain insight into the mechanism by which the cross-polarization response of the array antenna is generated. Also, a measure of the susceptibility of the antenna to cross-polarization effects, including such electronic counter measures (ECM) techniques as cross-polarization jamming, will be given as a function of phase shifter characteristics.

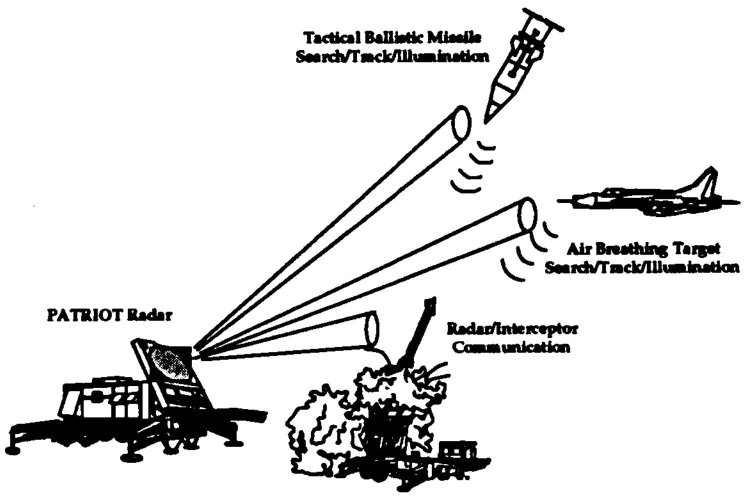

Figure 1.1. Phased array as utilized by the PATRIOT missile system

B. BACKGROUND INFORMATION

A phased array antenna typically consists of a large number of radiating elements called phase shifters placed in a grid configuration. Each element radiates radio-frequency (RF) energy with controlled amplitude and phase. The design engineer chooses the amplitude, phase, and geometric positioning of each radiating element to produce the desired antenna characteristics (.ie., beam width, side lobe level, and beam pointing angles).[3,4]

The beam of an array antenna can be scanned off boresight by applying a linearly distributed phase shift to the RF energy radiating from each element. The amount of phase shift induced is proportional to the desired scan angle.[5]

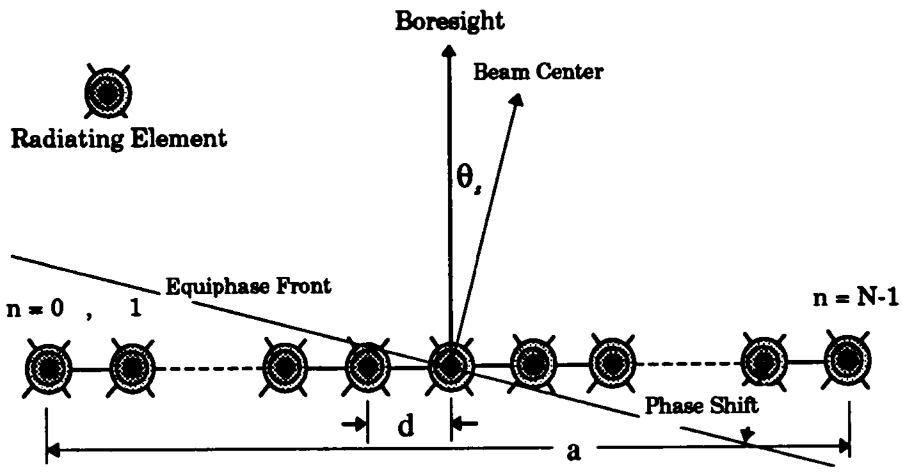

Figure 1.2. Linear phased array scanned θ_s degrees off boresight

Figure 1.2 shows a linear array scanned θ_s degrees off boresight. The RF energy from each element is being radiated with a phase such that the vector sum is constructive in the direction θ_s degrees off boresight. Hence, the array's main beam is steered θ_s degrees off boresight. The phase component that each element must induce is equal to

$$shift(n) = \frac{2\pi nd}{\lambda}\sin\theta_s\,, \tag{1.1}$$

where n is the element number and d is the element spacing.

In the space fed phased array, each element is a passive device that induces a phase shift in the propagating wave (see Figure 1.3). The collective array serves much like a lens to focus the RF energy.

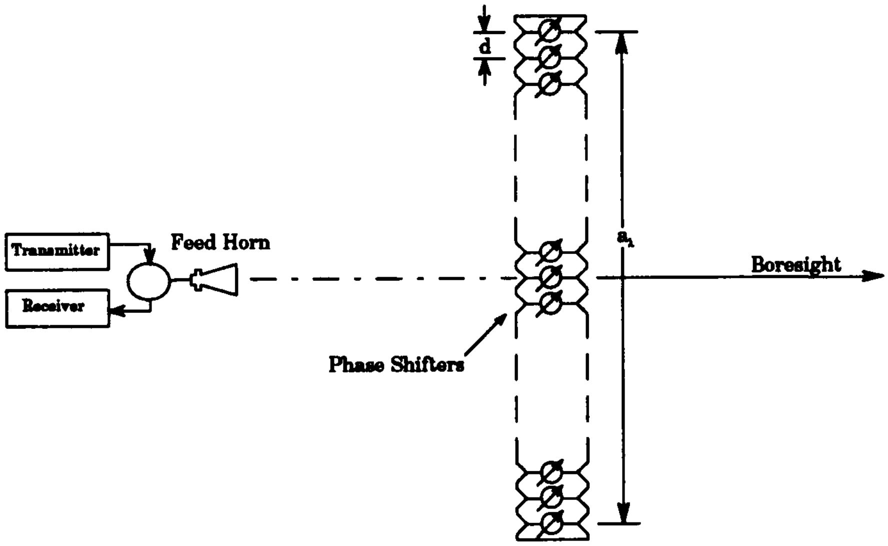

Figure 1.3. Space fed linear array. Adapted from Skolnik, Merrill. Radar Handbook, Second Edition. New York: McGraw Hill Publishing Co., 1990.

This analysis will focus on the evaluation of antenna sum and difference patterns produced by an array antenna with a monopulse feed configuration. (see Figure 1.4)

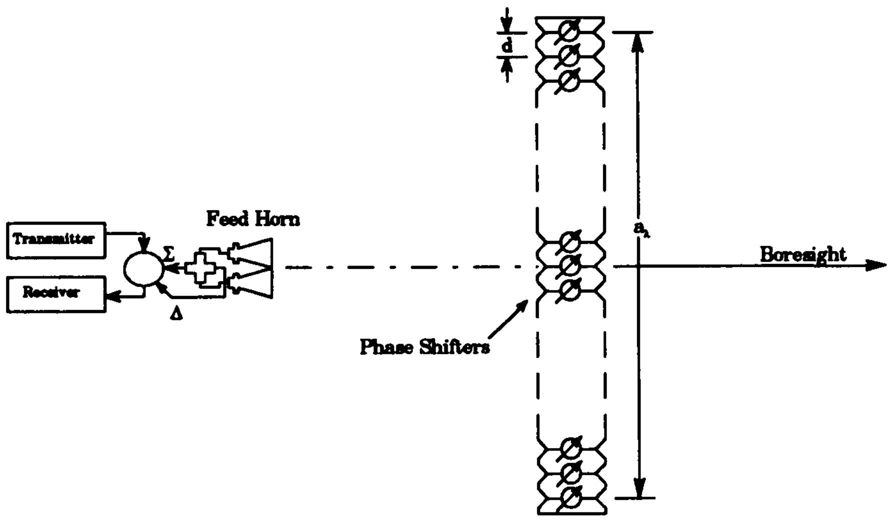

Figure 1.4. Monopulse antenna configuration. Adapted from Skolnik, Merrill. Radar Handbook, Second Edition. New York: McGraw Hill Publishing Co., 1990.

Each feed horn effectively produces an antenna beam. Due to geometric positioning of the feed horns, the two beams are slightly offset, or squinted. Patterns one and two are added, and subtracted to produce sum and difference patterns such as that shown in Figure 1.5.

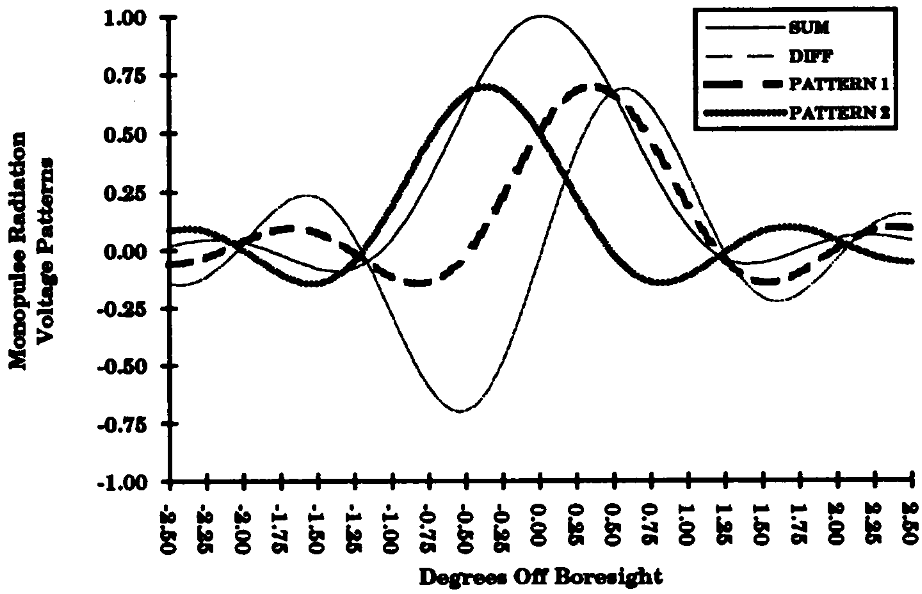

Figure 1.5. Squinted monopulse beams

There are basically two different types of phase shifters: ferrite and diode devices.[6] This paper focuses on ferrite phase shifters and their role in determining the cross-polarization response of an array antenna.

The array antenna studied here consists of circularly polarized ferrite phase shifters. The phase shifter geometry is that of a Faraday rotator with a ferrite rod located at the center of a circular waveguide with a longitudinally applied magnetic field as shown in Figure 1.6.

Circularly polarized waves entering the guide are rotated by an amount proportional to the magnetic field induced by the external solenoid. The phase shifts will be different for both right-hand (RH) and left-hand (LH) polarization.[7,8] Because of the non-reciprocal nature of the device, two separate antenna patterns may be generated; one for the RH circular polarization, and one for the LH circular polarization.

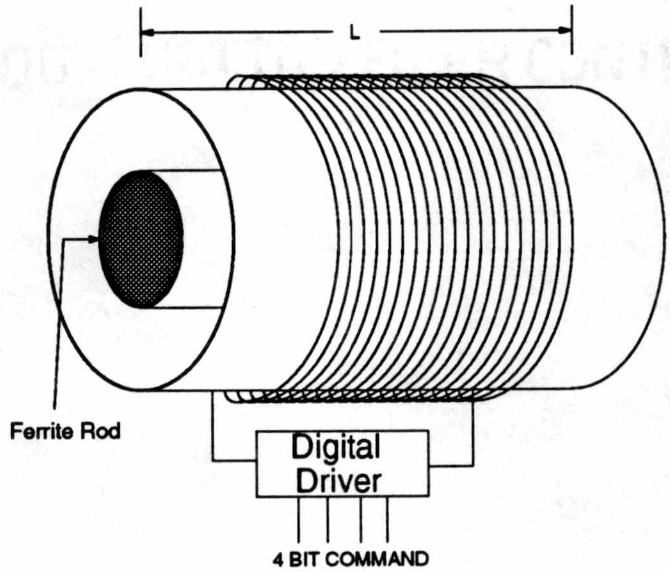

Figure 1.6. Circularly polarized ferrite phase shifter

Reciprocality of a device refers to a comparison of the phase shift induced in the energy propagating in opposite directions through the device. When one sense of polarization receives the same phase shift regardless of direction of propagation, the device is said to be reciprocal. Likewise, when phase shift is dependent on direction of propagation, the device is non-reciprocal.[6] The phase shifter to be modeled in this paper is non-reciprocal.

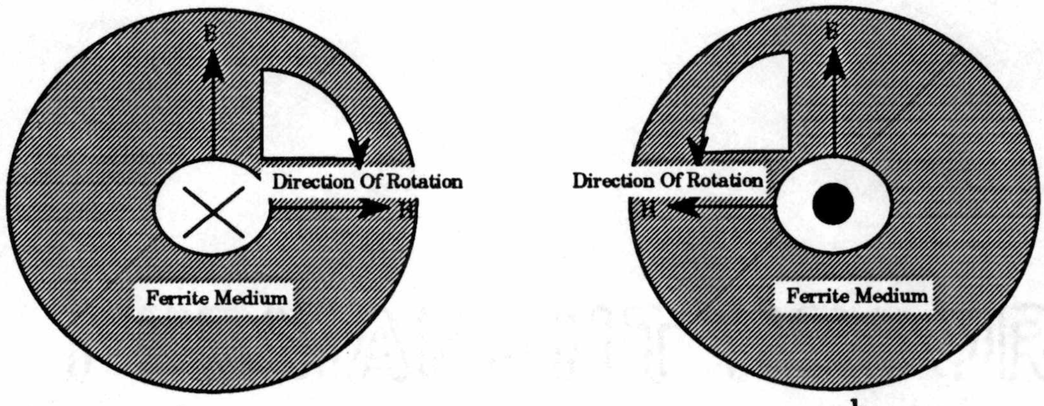

a. b.

Figure 1.7. RH circularly polarized energy propagating in opposite directions through a ferrite medium

The polarization characteristics, in the most general sense, can be derived intuitively for this device. First consider a RH circularly polarized wave entering the phase shifter as shown in Figure 1.7a. The electromagnetic field receives a phase shift of ϕ_1 as it propagates through the ferrite medium, rotating in a clockwise fashion. On the other hand, a RH circularly polarized wave traveling in the opposite direction, as shown in Figure 1.7b., receives a phase shift of ϕ_2 and has a counterclockwise rotation when viewed from the same perspective.

The same argument holds true for LH circularly polarized waves. Figure 1.8a and Figure 1.8b shows a representation of LH circularly polarized waves propagating in opposite directions through the phase shifter. Here, the energy propagating into the device has a counterclockwise rotation and thus receives a phase shift of ϕ_2, and the energy propagating in the opposite direction receives a phase shift ofϕ_1.

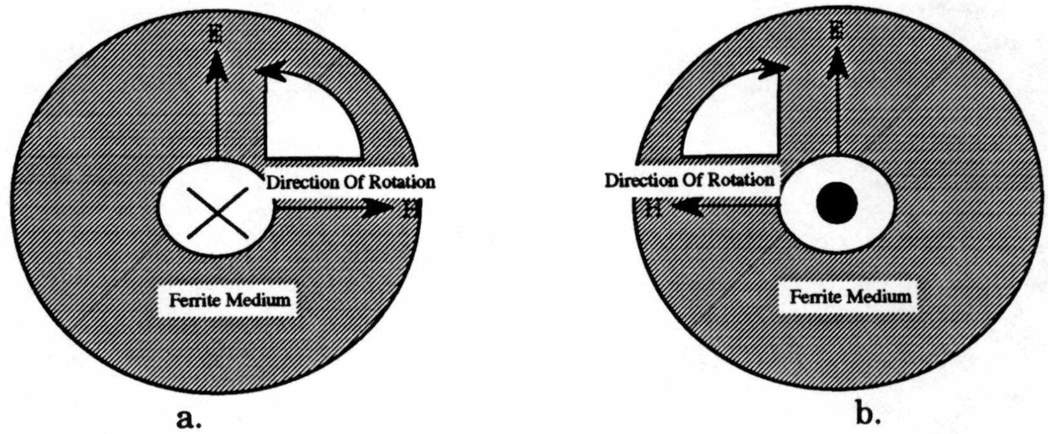

Figure 1.8. LH circularly polarized energy propagating in opposite directions

Figure 1.9 shows a summary of the phase shift induced in RH and LH polarizations for transmit and receive through a simple Faraday rotator phase shift. The arrows represent the direction of propagation through the device.[6] The means by which ϕ_1 and ϕ_2 are calculated will be discussed later in chapter 2.

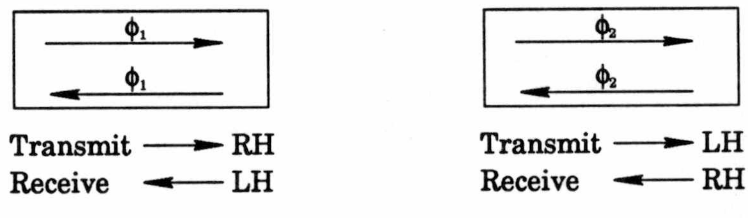

Figure 1.9. Polarization characteristics of a simple circularly polarized Faraday rotator type ferrite medium

CHAPTER II

ANTENNA MODEL DEVELOPMENT

A. COORDINATE SYSTEM

The first step in the development of the antenna model is to define an appropriate coordinate system.[8] It is generally considered standard to place the array antenna in the center of a sine-space coordinate system. This allows the antenna beam, and the effect of scanning to be visualized as the projection onto a planar surface as shown in Figure 2.1.

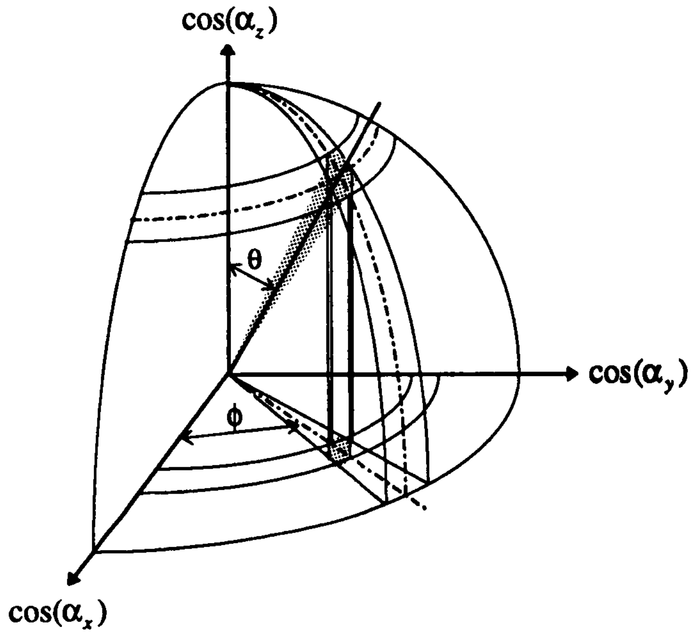

Figure 2.1. Sine-space coordinate system. Adapted from Skolnik, Merrill. Radar Handbook, Second Edition. New York: McGraw Hill Publishing Co., 1990.

The array is oriented such that the Z axis is perpendicular to the front face of the array, and the X axis is in the horizontal direction (Figure 2.2).

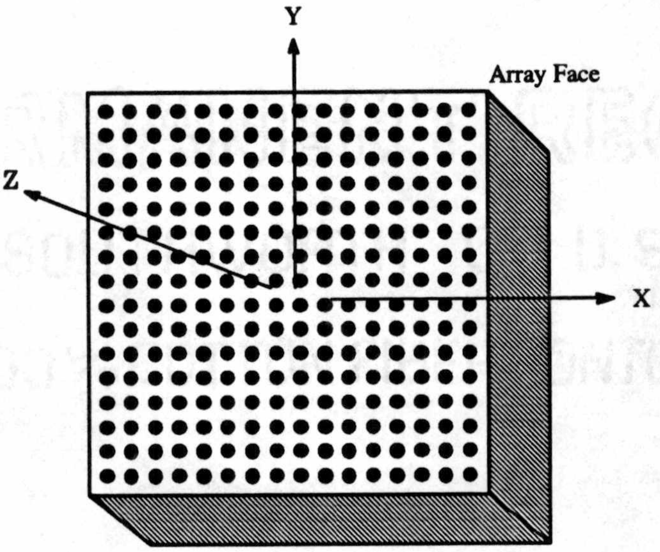

Figure 2.2. Array/axis orientation.

For any point on the unit sphere, the direction cosines are given by

$$\begin{aligned} \cos(\alpha_z) &= \cos(\theta) \\ \cos(\alpha_x) &= \sin(\theta)\cos(\phi) \\ \cos(\alpha_y) &= \sin(\theta)\sin(\phi) \end{aligned} \qquad \textbf{(2.1)}$$

B. PHASE SHIFTER DISCRETIZATION ERRORS

The phase shifter discretization errors have significant effects on the formation of radiation patterns, therefore will be included in the model.[9]

The radiating elements are Faraday rotator type ferrite devices with digital driver circuits. The drivers control the amount of current supplied to a solenoid located external to the wave guide thus controlling the applied magnetic field. This in turn regulates the phase shift induced in the propagating wave. The phase shifter drivers typically receive a four bit command. As a result, significant discretization errors are introduced into the phase settings. Figure 2.3 shows the sixteen discrete achievable phase shift settings for a four bit driver vs. applied magnetic field. Any desired phase shift that falls between these discrete settings will be discretized, thus producing a discretization error.

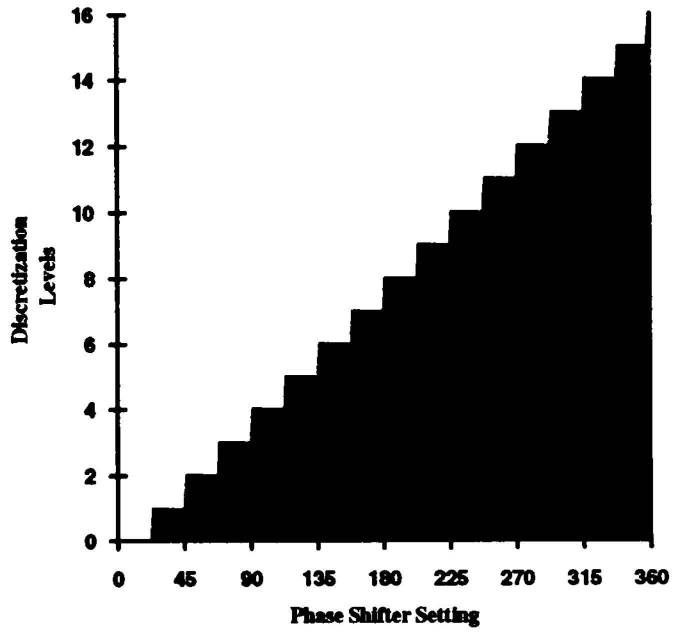

Figure 2.3. Sixteen discretization levels for a four bit phase shifter.

For example, if a phase shifter setting of τ is desired, the actual phase shift induced is given by

$$D[\tau] = \text{integer}\{\frac{\sigma \cdot 16}{2\pi}\} \cdot \frac{2\pi}{16} \quad . \tag{2.2}$$

C. QUADRATIC PHASE DISTRIBUTION

The antenna under consideration is a space feed array. Electromagnetic energy is passed from a feed horn to an array of phase shifters as shown in Figure 2.4. The array is geometrically located in the near field of the feed, resulting in a quadratic phase distribution that must be compensated for in the phase shifter commands.[3]

For a one dimensional array, the phase shifter setting required to compensate for the quadratic phase distribution is given by:

$$T_Q(n) = \sqrt{f^2 + r_o^2} - \sqrt{f^2 + r_n^2} \tag{2.3}$$

where, f = Closest distance from the feed horn to the array
r_n = Distance from the center of the array to the n^{th} element.

For the two dimensional case, r_n is replaced with $\sqrt{r_n^2 + r_m^2}$. Equation 2.3 becomes

$$T_Q(m,n) = \sqrt{f^2 + r_{no} + r_{mo}} - \sqrt{f^2 + r_n + r_m} \quad . \tag{2.4}$$

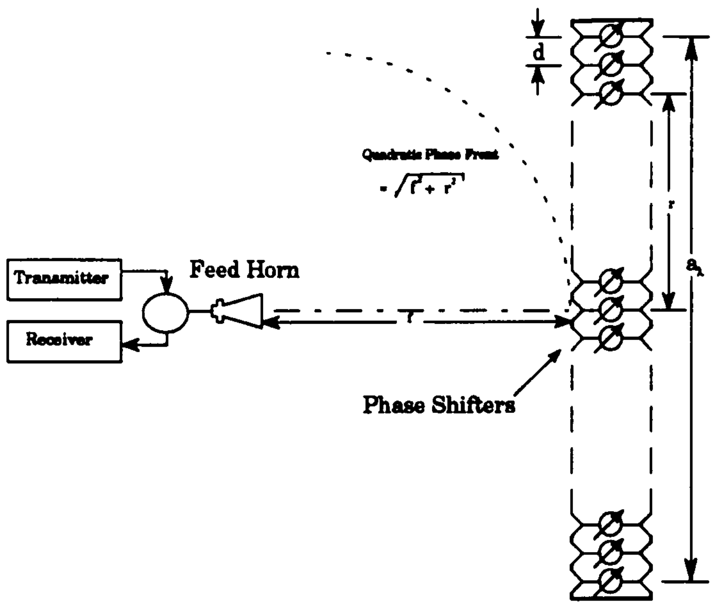

Figure 2.4. Space feed phased array. Adapted from Skolnik, Merrill. Radar Handbook, Second Edition. New York: McGraw Hill Publishing Co., 1990.

For example, if we wish to apply a linear phase shift across an array, as shown in Figure 2.5a, we must in fact apply a phase shift similar to that shown in Figure 2.5b to compensate for the quadratic phase distribution associated with the feed horn.

Figure 2.6 shows the phase errors introduced by the digital phase shifters. In this case, the antenna beam is at zero degrees off boresight, however the phase shifters are set to compensate for the quadratic phase distribution introduced by the feed horn configuration. Note that phase errors of up to .075 radians, or 4.3 degrees generated.

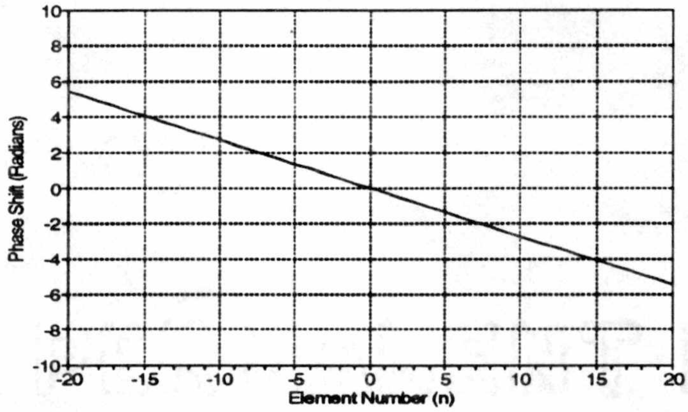

a.

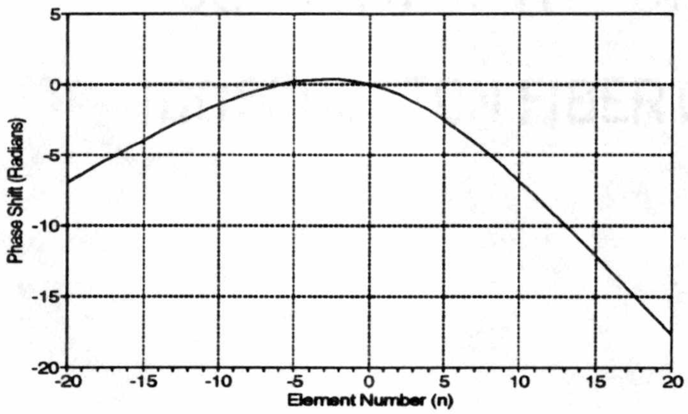

b.

Figure 2.5. Phase distribution required to steer the beam θ_s off boresight with, and without compensation for the quadratic phase distribution

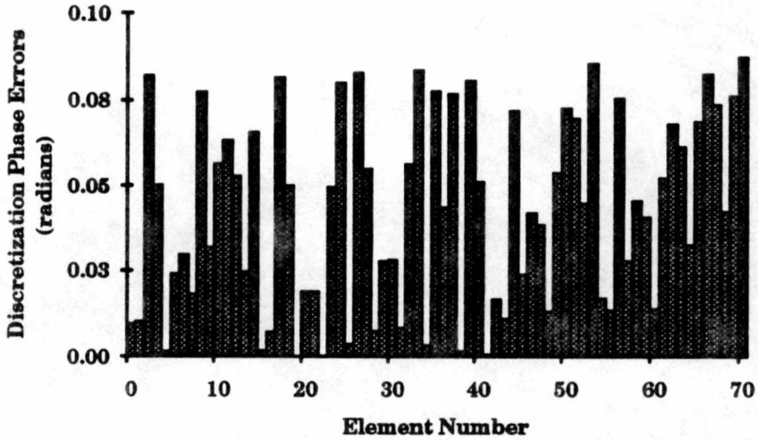

Figure 2.6. Phase errors introduced by the digital phase shifters

D. POLARIZATION CHARACTERISTICS OF A FERRITE MEDIUM

As electromagnetic, or RF energy propagates through a medium other than free space, it will suffer attenuation at a rate highly dependent on its frequency. For example, as 30 giga hertz RF energy propagates through the troposphere, it is attenuated at a rate of approximately .05 decibel per nautical mile; 3 giga hertz on the other hand, is attenuated at only .006 decibels per nautical mile in earth's troposphere[9]. The speed at which RF energy propagates through a medium is also dependent on frequency. RF energy can be passed through a medium with a slower propagation speed for a precise distance, thus effectively shifting its phase. These properties are characterized in the propagation constant for the medium.

Ferrite has the unique property of being able to slow the velocity of propagation, or shift phase, without inducing large attenuations. Also, these properties can easily be changed by applying a direct-current (dc) magnetic field to the ferrite. According to Lax and Button[7], the propagation constant ($\Gamma_{\pm}$) is a complex quantity, whose real part ($\alpha_{\pm}$) is defined as the attenuation constant, and whose imaginary part ($\beta_{\pm}$) is defined as the phase constant. The ± subscript denotes the propagation constants for co and cross -polarizations.

Equation 2.5 defines the relationship between the propagation constant and the electric field ($\boldsymbol{E}$), assuming that the applied magnetic field is parallel to the direction of propagation.

$$\boldsymbol{E} = \boldsymbol{E}_o e^{-\Gamma z} \tag{2.5}$$

where E_0 represents the electric field in free space.

Mathematical modeling of the polarization response of a partially filled circular wave guide involves solving Maxwell's equations with the appropriate boundary conditions. Lax and Button[6] derive the attenuation and phase constants for a thin ferrite rod in a circular wave guide as:

$$\beta_\pm = \beta_0[1 + A\frac{\Delta S_l}{S_l}(\chi''_\pm + \chi_e^{eff})]$$

(2.6)

and,

$$\alpha_\pm = \beta_0 A \frac{\Delta S_l}{S_l}\chi'_\pm \qquad (2.7)$$

where	β_0	=	dielectric constant $=\frac{\omega}{c} = \sqrt{\omega^2 \varepsilon_0 \mu_0}$
	A	=	2.1 for circular wave guide
	$\Delta S_l / S_l$	=	loading factor, or percent filled
	χ_e^{eff}	=	effective susceptibility[8]
	$\chi'_\pm$	=	dispersive part of susceptibility
	$\chi''_\pm$	=	dissipative part of susceptibility

Figure 2.7. shows $\beta_\pm$ calculated for a wave guide partially filled with M-O42 ferrite [7]. Note that for the region from 0 to 2000 oersteds, β_+ and β_- are approximately linear with opposite slopes.

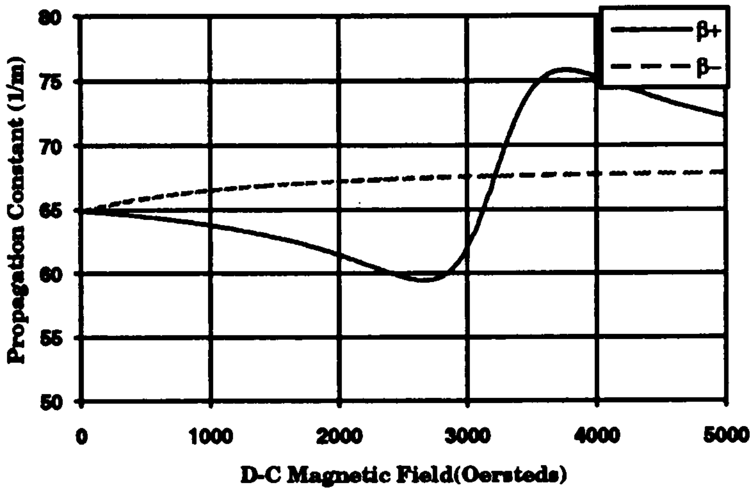

Figure 2.7. Calculated phase constant for M-042 in a 3% filled wave guide

$\beta_{\pm}$ has the units radians/meter. Therefore, for a given distance l, the phase shift induced, or insertion phase is given by

$$Phase\ Shift_{\pm} = \beta_{\pm} \cdot l. \qquad \textbf{(2.8)}$$

Figure 2.8. shows the insertion phase measured by Corey[12], from actual phase shifters in this configuration. Insertion phase refers to the actual phase shift induced into the wave as it propagates through the device. The phase state refers to the desired phase setting, and is directly proportional to the externally applied magnetic field. Appendix A shows $\alpha_{\pm}$ and $\beta_{\pm}$ calculated for various ferrite materials in a 3% partially filled wave guide. One should note that the designer, through material selection, has some degree of flexibility concerning the polarization

characteristics of the phase shifter, and consequently that of the array antenna.

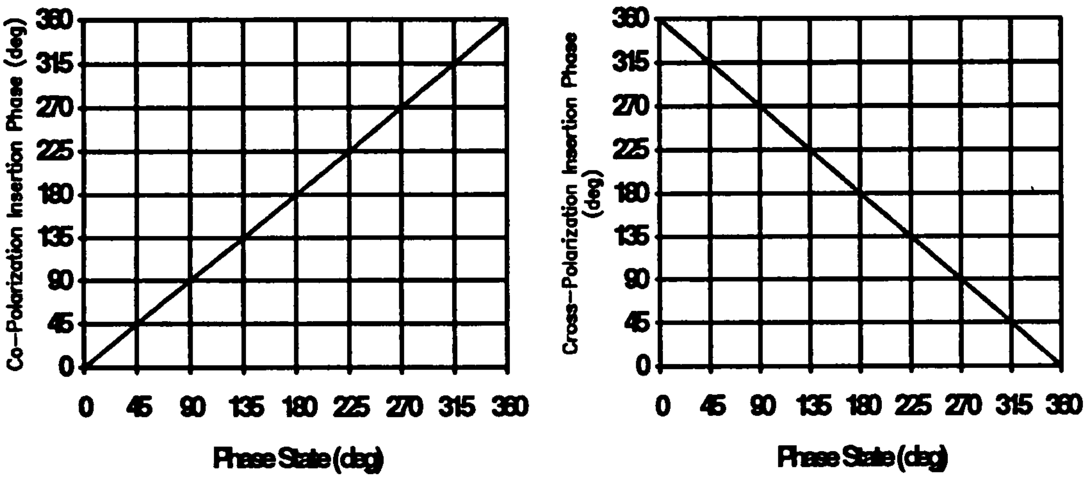

Figure 2.8. Measured insertion phase. Source: Williams, S. P. and L. E. Corey. "Polarization Characteristics of Phased-Array Antennas Using Circularly Polarized Dual-Mode Ferrite Phase Shifters." Final Report from the Georgia Institute of Technology.

E. ARRAY MODEL

According to Kraus[3], the far field radiation pattern $E(\theta)$ produced by a finite continuous one dimensional aperture can be written as:

$$E(\theta) = \int_{-a/2\lambda}^{a/2\lambda} A(x) e^{j2\pi x \sin(\theta)} dx \qquad \textbf{(2.9)}$$

where	λ	=	wavelength
	a	=	aperture or antenna length
	$A(x)$	=	illumination function.

Figure 2.9. depicts a parabolic reflector antenna being illuminated by a feed horn. The distribution of RF energy across the antenna face is referred to as the illumination function. The feed horn can be designed to produce various illumination functions which define the characteristic parameters of the antenna.

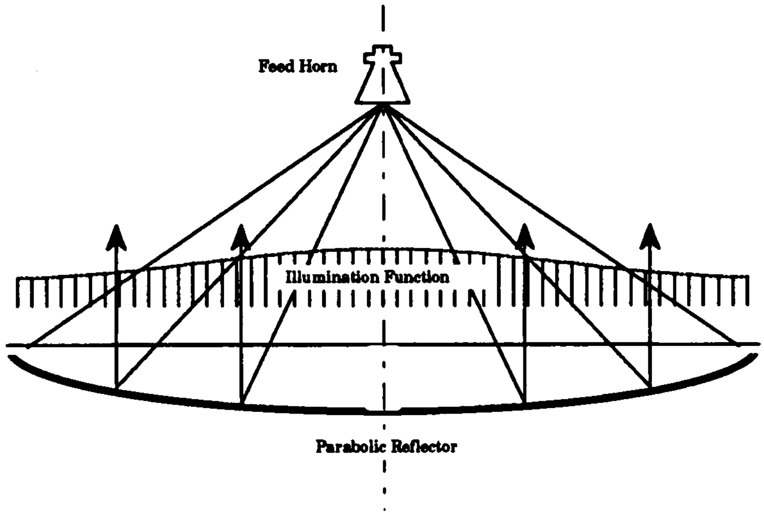

Figure 2.9. Parabolic reflector antenna and illumination function

Note that in equation 2.5, the illumination function ($A(x)$) is a real function. Therefore, there is no means by which to electrically steer the antenna beam off boresight. In this case, the antenna structure must be rotated and pivoted to move the antenna beam in two dimensional space.

The illumination function provides a great deal of flexibility in the placement of desired characteristics into a radiation pattern. Figure 2.10 shows the radiation patterns $E(\theta)$ associated with several different illumination functions.

Using the uniform illumination as a reference, the more tapered distributions (triangular and cosine) have larger beam widths and smaller sidelobes, while the most gradually tapered distribution (cosine squared) has yet a larger beam width and lower sidelobes. An aperture with uniform illumination will produce the largest gain, or directivity of all the distributions. However, the first sidelobe is only approximately 13 decibels (dB) below the main lobe. In practical systems, the illumination function provides a mechanism for tradeoff between beam width and sidelobe level.[5]

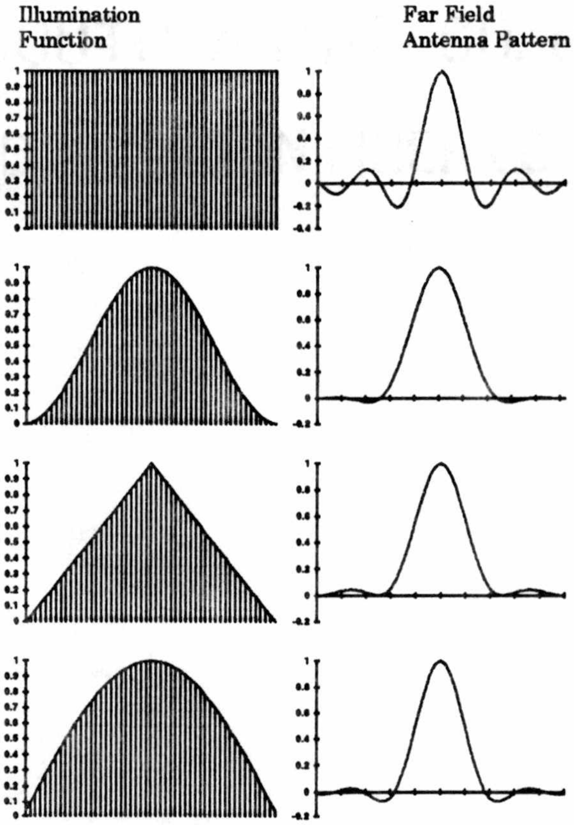

Figure 2.10. Illumination functions with their associated Fourier transform. Adapted from Kraus, John D. Antennas, Second Edition. New York: Mcgraw-Hill Book Company, Inc., 1988.

For non-continuous apertures, or array antennas, the far field radiation pattern can be written as the sum of the individual contributors.[9] The one dimensional solution is

$$E(\theta)=\sum_{n=0}^{N-1}A(n)e^{\frac{j2\pi nd\sin\theta}{\lambda}} \tag{2.10}$$

where	N	=	Total number of phase shifters
	d	=	Element spacing
	A(n)	=	illumination function

The radiation pattern of the array may be directed to an angle (θ_s) by applying a linearly distributed phase shift from element to element. The phase shift associated with the n^{th} element is given in equation 1.1. This phase component can be added to equation 2.10 to account for the phase shift induced by the phase shifters as follows:

$$E(\theta)=\sum_{n=0}^{N-1}A(n)e^{j[2\pi n\frac{d}{\lambda}(\sin\theta-\sin\theta_s)]} \tag{2.11}$$

As discussed in previous sections, the phase shift induced by each element can be precisely controlled to effectively steer the antenna beam off boresight.

Equation 2.10 may be expanded for the two dimensional case as follows:

$$E(\theta,\phi)=\sum_{m=0}^{M-1}\sum_{n=0}^{N-1}A(m,n)e^{j[m2\pi{}^{d_x}\!/_{\lambda}\sin\theta\cos\phi+n2\pi{}^{d_y}\!/_{\lambda}\sin\theta\sin\phi]} \tag{2.12}$$

where	M	=	number of rows
	N	=	number of columns
	d_x	=	Element spacing in rows
	d_y	=	Element spacing in columns
	A(m,n)	=	Illumination function

Note θ and ϕ are as defined in Figure 2.1.

As with the one dimensional case, an additional phase component can be added due to the phase shifters. If the scan angles are θ_s and ϕ_s then

$$Shift(m,n) = 2\pi \left(\frac{md_x}{\lambda} \sin\theta_s \cos\phi_s + \frac{nd_y}{\lambda} \sin\theta_s \sin\phi_s\right), \tag{2.13}$$

and equation 2.12 becomes[9]

$$E(\theta,\phi) = \sum_{m=0}^{M-1} \sum_{n=0}^{N-1} A(m,n) e^{j[m2\pi \, {}^{d_x}/_{\lambda} (\sin\theta\cos\phi - \sin\theta_s \cos\phi_s) + n2\pi \, {}^{d_y}/_{\lambda} (\sin\theta \sin\phi - \sin\theta_s \sin\phi_s)]} . \tag{2.14}$$

One of the most commonly applied illumination functions is the cosine squared on a pedestal as shown in Figure 2.11. For a one dimensional array antenna, $A(n)$ is given by

$$A(n) = a_0 + a_1 \cos^2\left(\frac{\pi n}{N-1}\right) \tag{2.15}$$

where	a_0	=	Uniform distribution amplitude
	a_1	=	Cosine squared distribution amplitude
	n	=	Element number.

If the illumination function in Figure 2.11 is centered, and then rotated around the z axis, the two dimensional illumination function is given by;

$$\begin{aligned} &if\ \frac{\sqrt{m^2+n^2}}{N-1} \le 1, \quad A(m,n) = a_0 + a_1 \cos^2\left(\frac{\pi\sqrt{m^2+n^2}}{N-1}\right) \\ &if\ \frac{\sqrt{m^2+n^2}}{N-1} > 1, \quad A(m,n) = a_0 \end{aligned} \quad . \qquad \textbf{(2.16)}$$

The cosine squared distribution is usually combined with the uniform distribution in variable ratios to provide the desired antenna pattern.

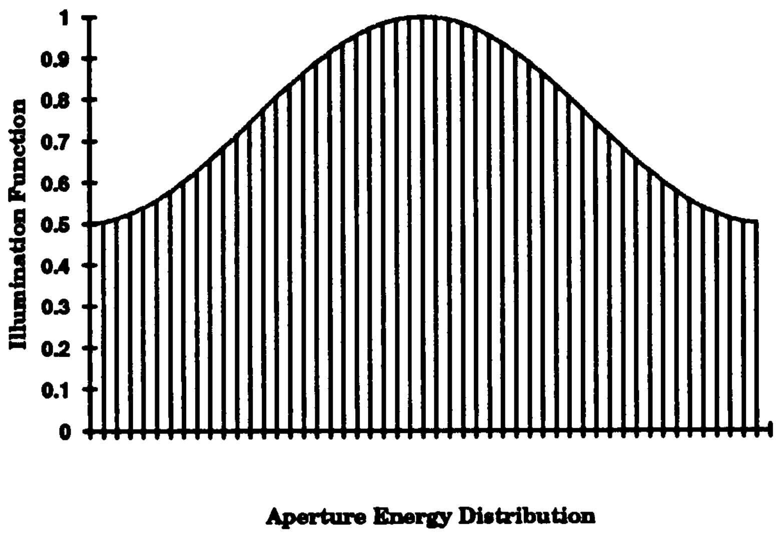

Figure 2.11. Cosine squared on a pedestal illumination function.

One effect of scanning the beam off boresight is to effectively reduce the aperture to the size of its projection normal to the scan angle (see

Figure 2.12). This results in an increase in the beam width, thus a reduction in gain proportional to the cosine of the scan angle.[5]

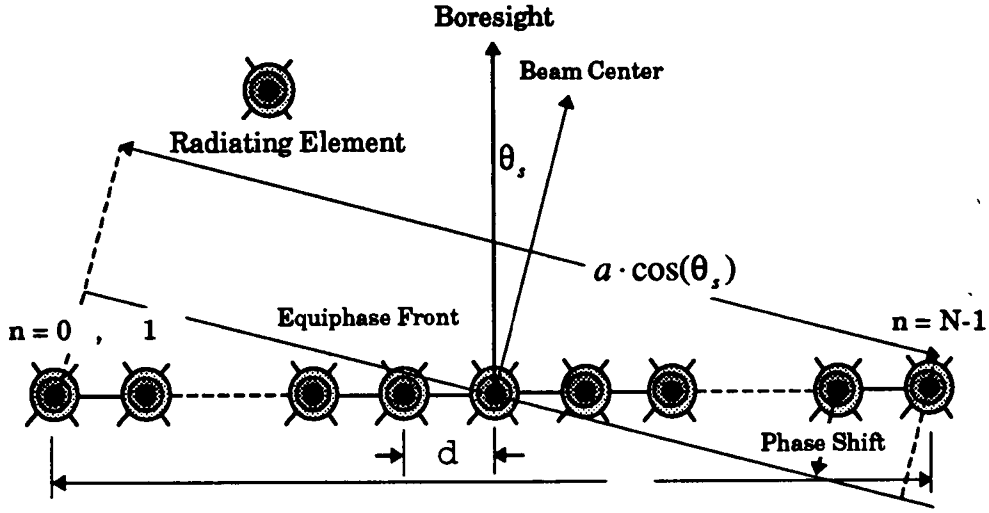

Figure 2.12. Linear array scanned $\theta_s$deg. off boresight

In the preceding discussion, the radiating elements were assumed to be isotropic. Antenna patterns generated under this assumption are generally referred to as array patterns($E_a(\theta)$). In reality each radiating element has associated with it a radiation pattern called the element factor, or element pattern ($E_e(\theta)$).

The total radiation pattern in the far field is then approximated by the product of the array factor and the element factor;[9]

$$E(\theta) = E_a(\theta)E_e(\theta) \qquad \textbf{(2.17)}$$

For this analysis, the element factor was approximated as

$$E_e(\theta) = \cos(\theta). \tag{2.18}$$

Incorporating discretization errors, quadratic phase distribution, and element factor into equation 2.14 yields:

$$E(\theta,\phi) = \cos\theta \sum_{m=0}^{M-1}\sum_{n=0}^{N-1} A(m,n)$$

$$\cdot\, e^{j[m\frac{2\pi d_x}{\lambda}(\sin\theta\cos\phi - T_Q(m,n)) + (n\frac{2\pi d_y}{\lambda}(\sin\theta\sin\phi - T_Q(m,n)) + shift_{co}(m,n)]}$$

(2.19)

where, the (m,n)th element of the array will induce the a phase shift of $shift_{co}(m,n)$ in the co-polarized wave, given by;

$$shift_{co}(m,n) = \frac{m2\pi d_x}{\lambda} D[\sin\theta_s \cos\phi_s + T_Q(m,n)] + \frac{n2\pi d_y}{\lambda} D[\sin\theta_s \sin\phi_s + T_Q(m,n)]$$

(2.20)

As discussed in the previous section, the phase shifters themselves support both right hand (RH), and left hand (LH) circular polarizations. However, the ferrite rod introduced into the wave guide presents different propagation constants for the two polarizations.[11] This data can be incorporated into the model such that both the co-polarization, and the cross-polarization patterns can be calculated

The phase shift induced in the cross-polarized wave is approximated as a linear function of $shift_{co}(m,n)$, and given as

$$shift_{cross}(m,n) = f\,(shift_{co}(m,n)) = shift_{co}(m,n) \cdot slope + 2\pi\,, \qquad \textbf{(2.21)}$$

where the variable "slope" refers to the slope of the phase shifter insertion phase curve (e.g., Figure 2.8). For the cross-polarization case, equation 2.19 becomes

$$E_{cross}(\theta,\phi) = \cos\theta \sum_{m=0}^{M-1}\sum_{n=0}^{N-1} A(m,n)$$

$$\cdot\, e^{j[m\frac{2\pi d_x}{\lambda}(\sin\theta\cos\phi - T_Q(m,n)) + (n\frac{2\pi d_y}{\lambda}(\sin\theta\sin\phi - T_Q(m,n)) + shift_{cross}(m,n)]}$$

(2.22)

The present model can easily be adapted to simulate a monopulse radar antenna by calculating separate radiation patterns in each orthogonal plane. This is accomplished by generating four patterns, as shown in Figure 2.13, and adding and subtracting them appropriately to produce the azimuth and elevation sum and difference patterns.

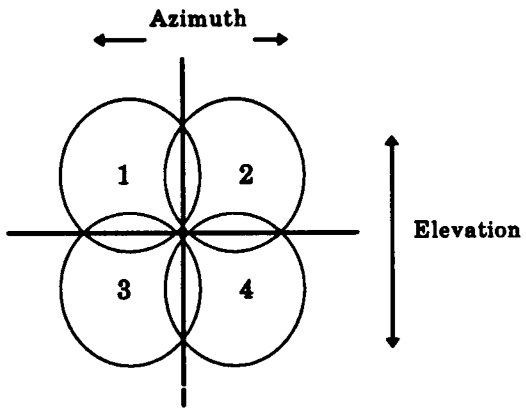

Azimuth:
$\Sigma = Pattern\,1 + Pattern\,2 + Pattern\,3 + Pattern\,4$
$\Delta_{AZ} = (Pattern\,1 + Pattern\,3) - (Pattern\,2 + Pattern\,4)$

Elevation:
$\Sigma = Pattern\,1 + Pattern\,2 + Pattern\,3 + Pattern\,4$
$\Delta_{EL} = (Pattern\,1 + Pattern\,2) - (Pattern\,3 + Pattern\,4)$

Figure 2.13. Monopulse azimuth, and elevation sum and difference patterns.

The cross-polarization and the co-polarizations azimuth radiation sum and difference patterns in one plane for a 45λ aperture are given in Figures 2.14 through 2.21 for various scan angles. The model under consideration uses a uniform energy distribution, and a linear approximation of the phase shifter's cross polarization response to match that measured by Corey.[12]

Note that for a zero scan angle the co and cross-polarization beams are effectively the same except for minor differences due to the discretization errors when compensating for the quadratic phase distribution (these minute differences cannot be detected in the Figures). However, as the antenna is scanned off boresight, the cross-polarization pattern becomes defocused rapidly as shown. In this case (recall Figure 2.8), the slopes of the insertion phase curves for co and cross-polarization have slopes of +1 and -1 respectively. In effect, Figure 2.17 shows the cross-polarization radiation pattern steering in the opposite direction.

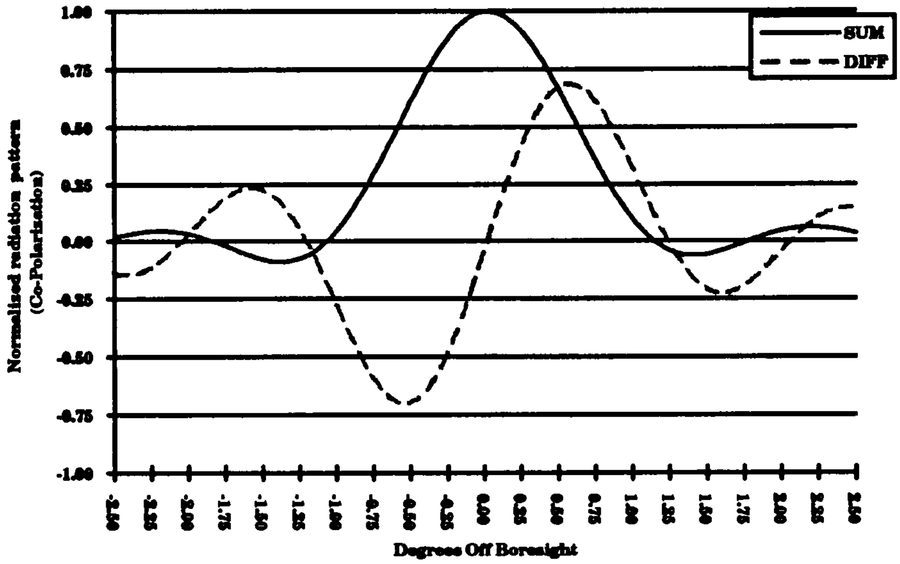

Figure 2.14. Co-polarization antenna pattern scanned 0 degrees off boresight

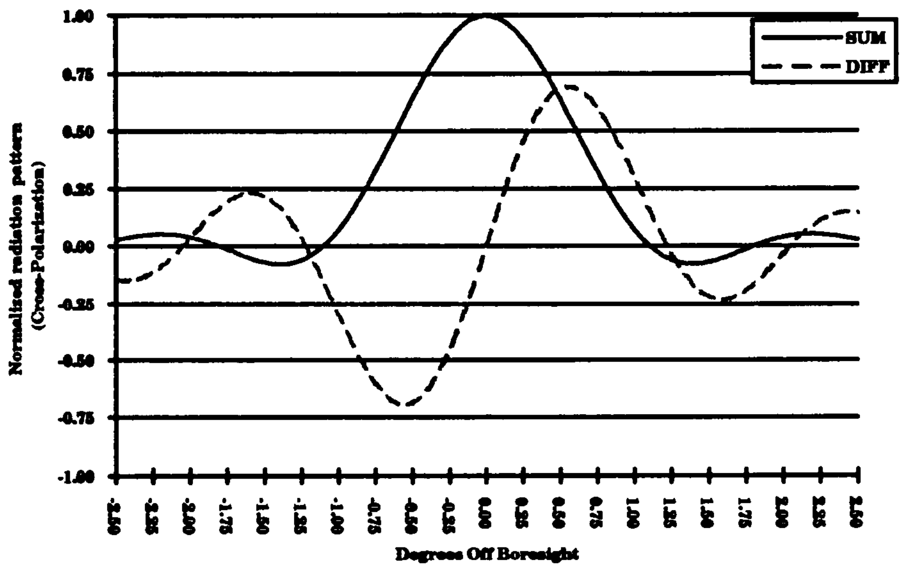

Figure 2.15. Cross-polarization antenna pattern scanned 0 degrees off boresight

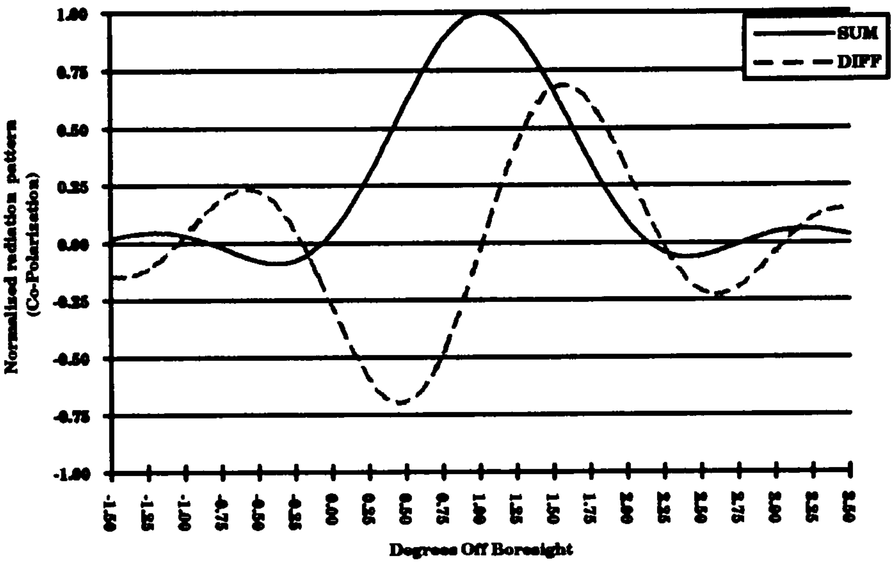

Figure 2.16. Co-polarization antenna pattern scanned 1 degrees off boresight

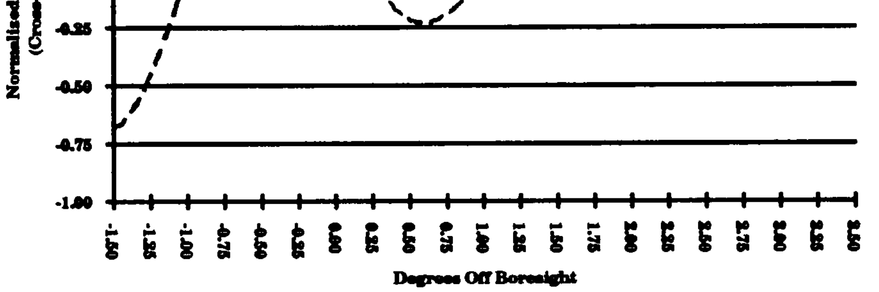

Figure 2.17. Cross-polarization antenna pattern scanned 1 degrees off boresight

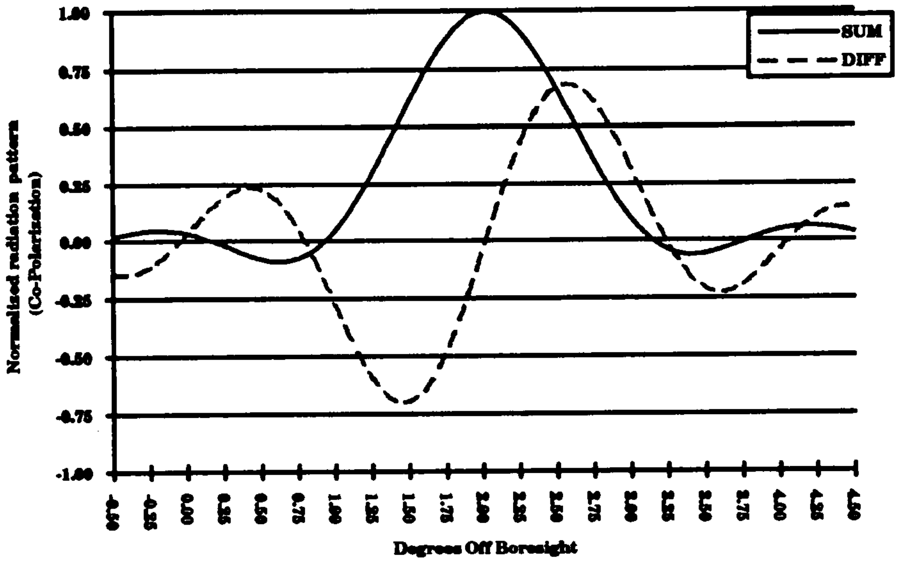

Figure 2.18. Co-polarization antenna pattern scanned 2 degrees off boresight

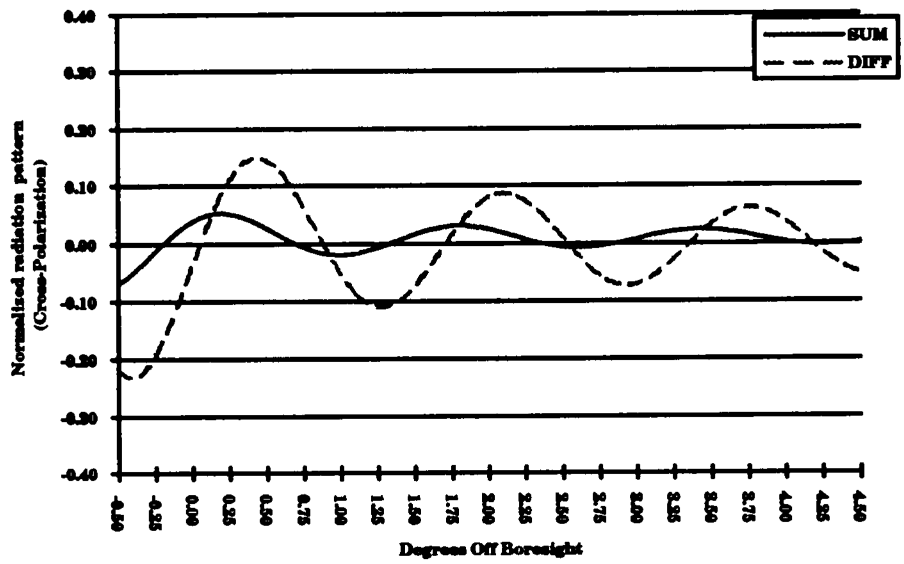

Figure 2.19. Cross-polarization antenna pattern scanned 2 degrees off boresight

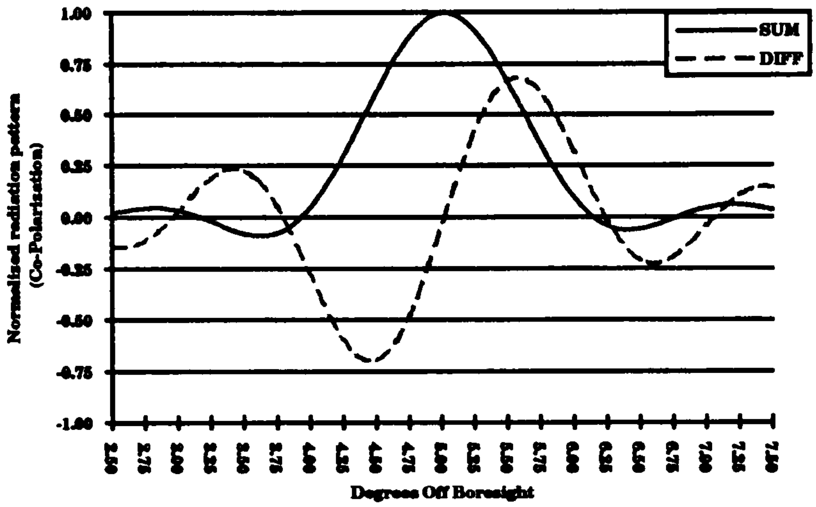

Figure 2.20. Co-polarization antenna pattern scanned 5 degrees off boresight

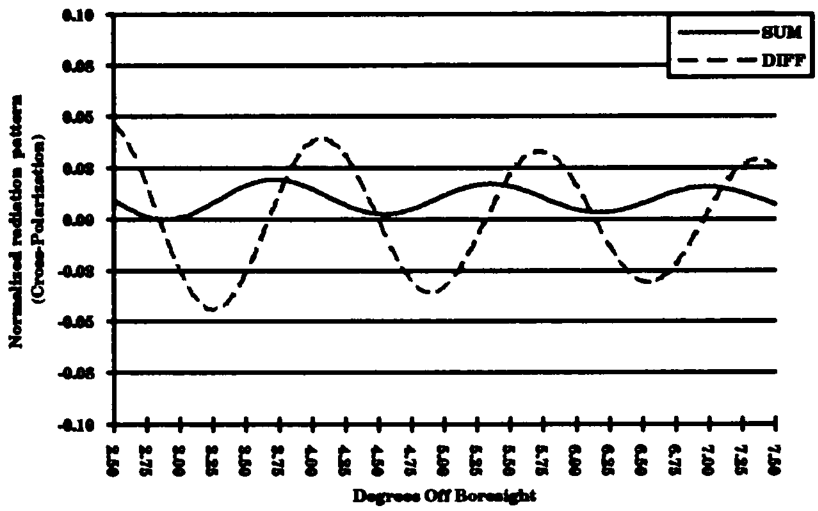

Figure 2.21. Co-polarization antenna pattern scanned 5 degrees off boresight

CHAPTER III

ANTENNA VULNERABILITY ANALYSIS

A. ANTENNA VULNERABILITY TO CROSS-POLARIZATION EFFECTS

If the target being tracked by a monopulse radar is not depolarized, as is generally the case with complex targets, then the radar antenna may experience angle tracking errors caused by the cross-polarization returns of the target itself. Another source of cross-polarization energy is an ECM technique appropriately called cross-polarization jamming.[13] In this type of ECM technique, the jammer detects the polarization of the victim radar and transmits the opposite polarization with the intention of causing large tracking errors, thus degrading the radar's ability to support a missile engagement.

To illustrate this phenomena, a relative measure of the cross-polarization error will be found for the antenna modeled in this paper (i.e., space fed phased array composed of four bit circularly polarized ferrite phase shifters with a cosine squared on a pedestal illumination function). This analysis will provide an illustrative display of potential cross-polarization "problem" spots in the antenna's scan area for various phase shifter designs.

B. VULNERABILITY TEST AND RESULTS

Having obtained the sum and difference patterns from the monopulse radar antenna model, the next goal for this study is to assess the antenna's vulnerability to cross-polarization effects assuming that the radar is designed to receive double bounce returns only. Recall that if one sense of circularly polarized waves are being transmitted, then each time the wave is reflected, it switches to the opposite polarization.[14] For example, if an antenna is transmitting RH circular polarized energy, then for "simple" targets, like spheres, the returning wave will have been reflected only once leaving it LH circularly polarized. Likewise, if the target is "complex", as are most targets of interest, there will be multiple paths of reflection, resulting in a return signal made up of both polarized signals.

In order to first establish a reference, assume the system only receives co-polarized returns. The angle sensing function, or monopulse ratio is given as follows by the ratio of the antenna difference pattern to the antenna sum pattern [17]:

$$REF = \frac{E_{OD}\sigma_O}{E_{OS}\sigma_O} = \frac{E_{OD}}{E_{OS}} \qquad \textbf{(3.1)}$$

where

σ_O = co-polarization Radar Cross Section (RCS)
E_{OD} = co-polarization difference E field
E_{OS} = co-polarization sum E field.

Figure 3.1 shows the calculated co-polarization monopulse ratio for the antenna under consideration. This curve defines the systems ability to accurately track a target in angle. For example, if the slope of the monopulse ratio is steep, small variations in target position would result in large fluctuations in the monopulse ratio. This scenario would maximize angular resolution, but as result minimize angular field of view. High angular accuracy may be achieved, but only at the expense of more frequent track updates. On the other hand, if the monopulse ratio slope is shallow, the angular accuracy would be minimized, but the angular field of view would be maximized. This may be desirable in a multi-function systems, where lower track rates are required. The important thing to note is that the monopulse ratio slope is determined by the geometric positioning of the feed horns with respect to the array face, thus at the discretion of the design engineer.

Equation 3.1 can be expanded to include the effects cross-polarized returns.[15] The monopulse ratio becomes

$$SENS = \frac{E_{OD}\sigma_O + E_{CD}\sigma_C}{E_{OS}\sigma_{OS} + E_{CS}\sigma_C} \qquad \textbf{(3.2)}$$

where σ_C = cross-polarization RCS
E_{CD} = cross-polarization difference E field
E_{CS} = cross-polarization sum E field

The next step in this analysis is to evaluate a scan area for susceptibility. In order to do this a particular target must be considered, and a considerable knowledge of the targets geometry, and RCS is required. This approach does not best serve the interest of this paper, where a more general analysis is desired.

The RCS information can be eliminated from the analysis entirely by making the substitution

$$\frac{\sigma_C}{\sigma_O} = \frac{J}{S} \tag{3.3}$$

where J = cross-polarization power
S = co-polarization power.

Now the antenna can be evaluated with simply a ratio of cross-polarization to co-polarization power. The angle monopulse ratio becomes[16]

$$SENS = \frac{E_{OD} + E_{CD}(J/S)}{E_{OS} + E_{CS}(J/S)} \tag{3.4}$$

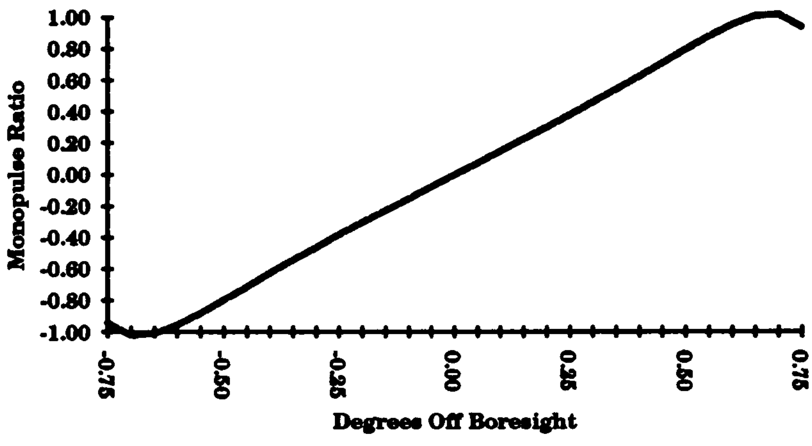

Figure 3.1. Co-polarization monopulse ratio

Recall Figures 2.13 through 2.20 showed that the cross-polarized antenna patterns were highly dependent on scan angle, while the co-polarized patterns remained fairly constant. It follows then that REF should remain constant throughout the scan area, and SENS should fluctuate greatly. Figures 3.2 through 3.5 show the calculated REF and SENS for various scan angles. Again, the phase shifter cross-polarization response was modeled after that measured by Corey[12].

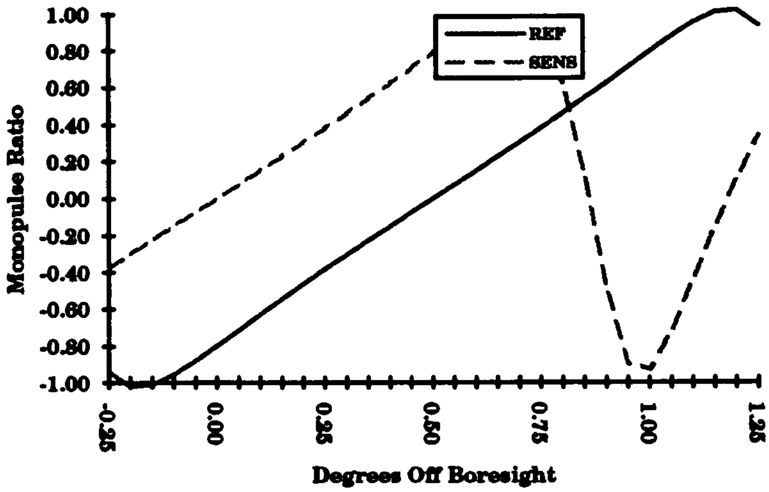

Figure 3.2. Monopulse ratio for array scanned .5 degrees off boresight

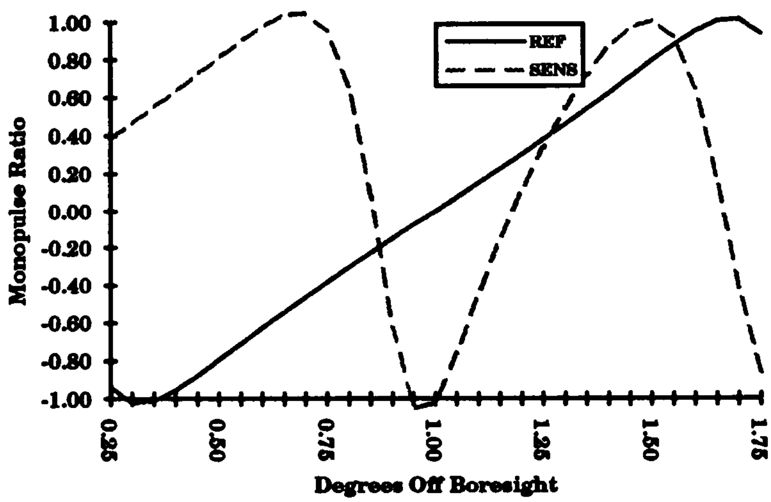

Figure 3.3. Monopulse ratio for array scanned 1 degree off boresight

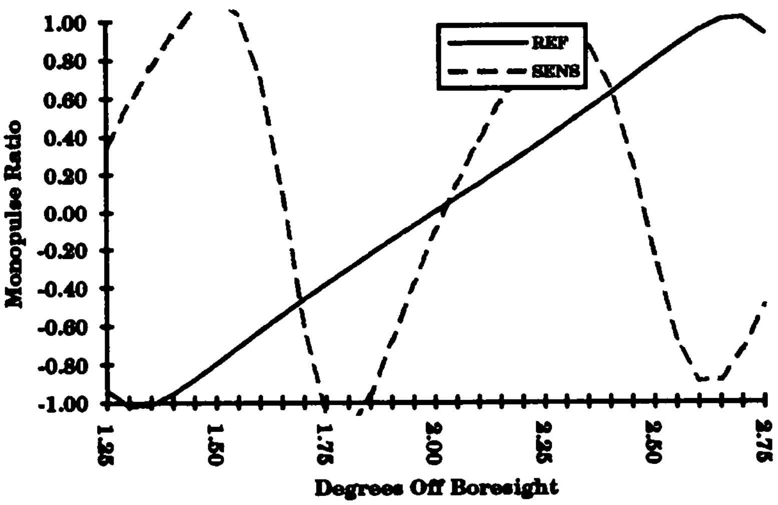

Figure 3.4. Monopulse ratio for array scanned 2 degrees off boresight

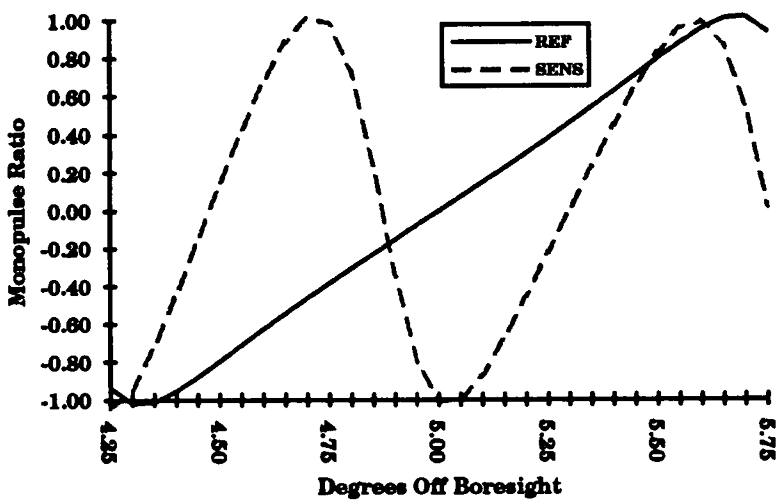

Figure 3.5. Monopulse ratio for array scanned 5 degrees off boresight

For the case where the antenna is scanned zero degrees off boresight, the co and cross-polarization ratios are essentially the same. A cross-polarization jammer would therefore introduce negligible tracking errors. However, for small distances off boresight, the monopulse ratios fluctuate greatly, potentially causing large tracking errors.

In order to evaluate the antenna for cross polarization jamming susceptibility, one must first establish a criteria for which the antenna's performance is acceptable or unacceptable. This criteria could be established through a detailed analysis of the system to include missile guidance and auto pilot responses. However, that is beyond the scope of the paper. For analysis purposes, a target will be placed ±.25 degrees off the beam center in the azimuth plane. If the monopulse tracking error (derived from the monopulse ratio) is greater that ±.25 degrees, it will be assessed as having effectively jammed the radar.

The susceptibility of the antenna model to cross-polarization jamming, as outlined above, will be evaluated at points in an approximately 20 deg. elevation by ± 20 deg. azimuth scan area. The array will be evaluated assuming phase shifters with cross-polarization response slopes of -1.0, -.95, -.90, -.80, +.90, +.95 and +1.0. In addition, the susceptibility is calculated for J to S ratios of 35 dB, 40 dB, and 45 dB. A relative measure of the susceptibility to cross-polarization jamming is obtained by dividing the number of points assessed to be effected by cross-polarization by the total number of points tested.

$$\delta = \frac{N_{pe}}{N_{pt}} \tag{3.6}$$

where δ = relative measure of susceptibility
N_{pe} = number of points assessed to be vulnerable
N_{pt} = number of points tested.

First consider the case where the slope of the cross-polarization response is the same as the co-polarization response (+1.0). The equiphase front of the cross-polarized wave will then naturally coincide with that of the co-polarized wave. In other words, the cross-polarization sum and difference patterns would be identical to the co-polarization sum and difference patterns. Phase shifters of this type would yield the array unaffected by cross-polarization jamming techniques. In fact the jammer would in effect become a beacon for the radar to track.

Next, if the cross-polarization response slope is set to +.97, it can be seen in Figures 3.6 through 3.8 that for over half of the antenna scan area, it is assessed as being susceptible to cross-polarization jamming. These Figures also indicate an insensitivity to jammer power.

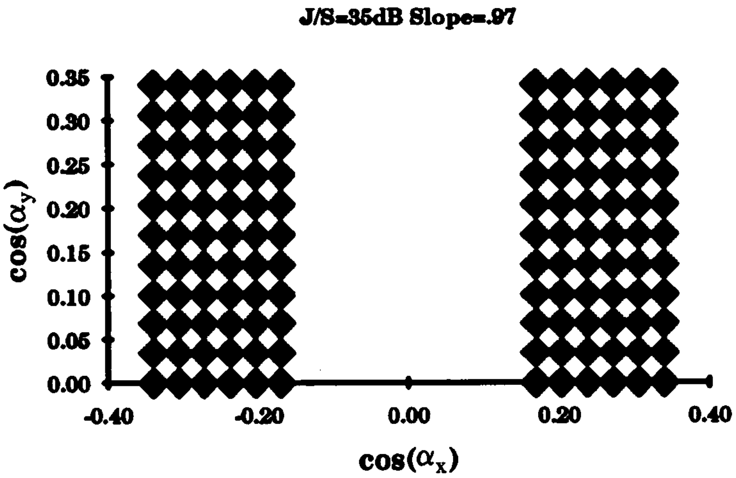

Figure 3.6. Scan area with a target located ±.25 degrees off beam center. J/S = 35 dB with the cross-polarization response slope equal to .97

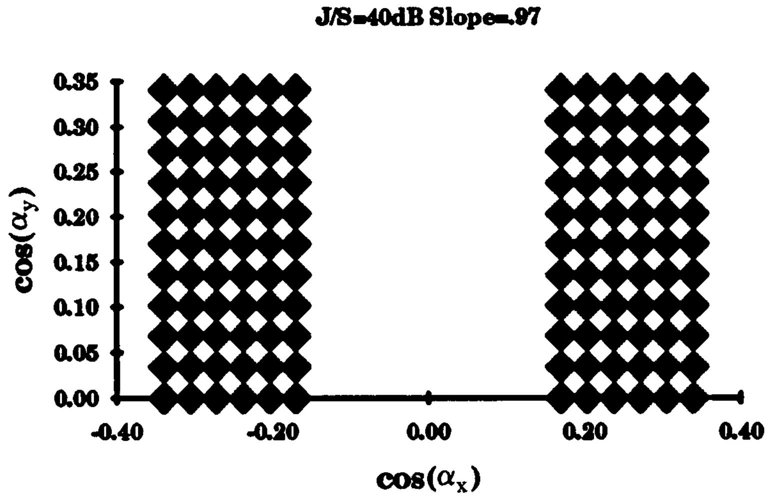

Figure 3.7. Scan area with a target located ±.25 degrees off beam center. J/S = 40 dB with the cross-polarization response slope equal to .97

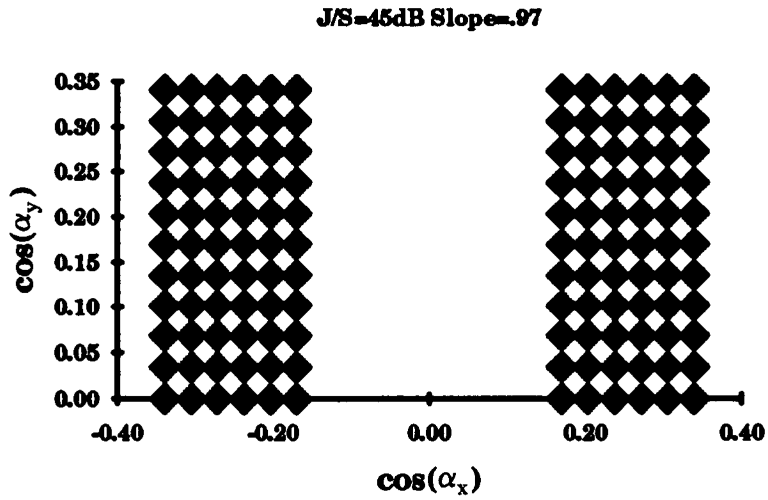

Figure 3.8. Scan area with a target located ±.25 degrees off beam center J/S = 45 dB with the cross-polarization response slope equal to .97

If the cross-polarization response slope is set to .95, Figures 3.9 through 3.11 show that for over 3/4 of the scan area, the antenna is susceptible to cross-polarization jamming. Again, antenna performance seems to be insensitive to jammer power.

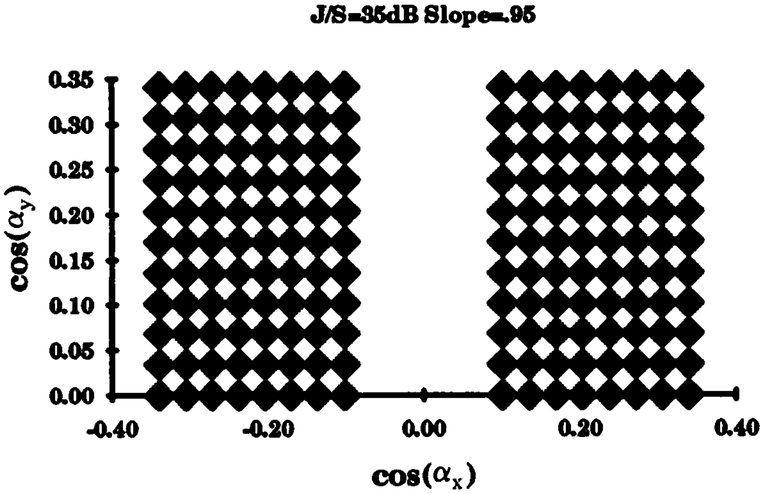

Figure 3.9. Scan area with a target located ±.25 degrees off beam center. J/S = 35 dB with the cross-polarization response slope equal to .95

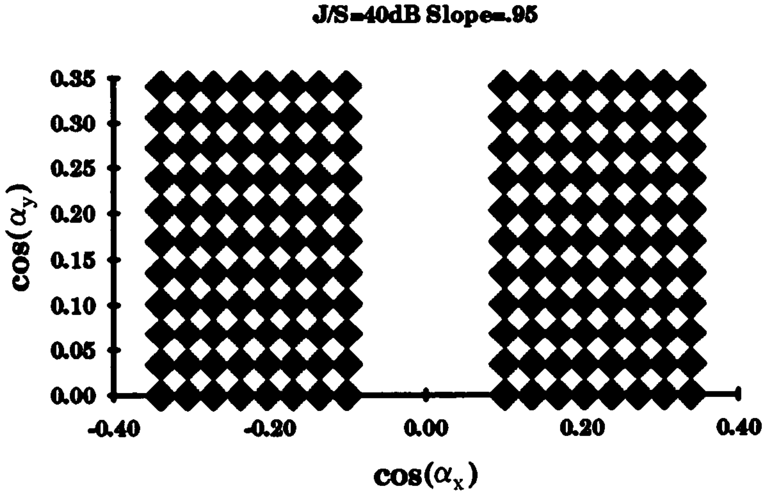

Figure 3.10. Scan area with targets located ±.25 degrees off beam center J/S = 40 dB with the cross-polarization response slope equal to .95

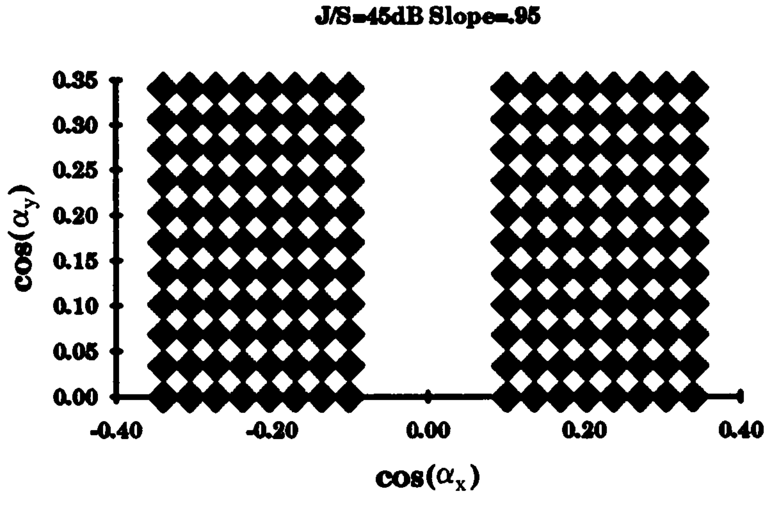

Figure 3.11. Scan area with a target located ±.25 degrees off beam center. J/S = 45 dB with the cross-polarization response slope equal to .95

As the cross-polarization response diverges farther from +1 to .9, the antenna becomes susceptible to cross-polarization jamming over almost the entire scan area.

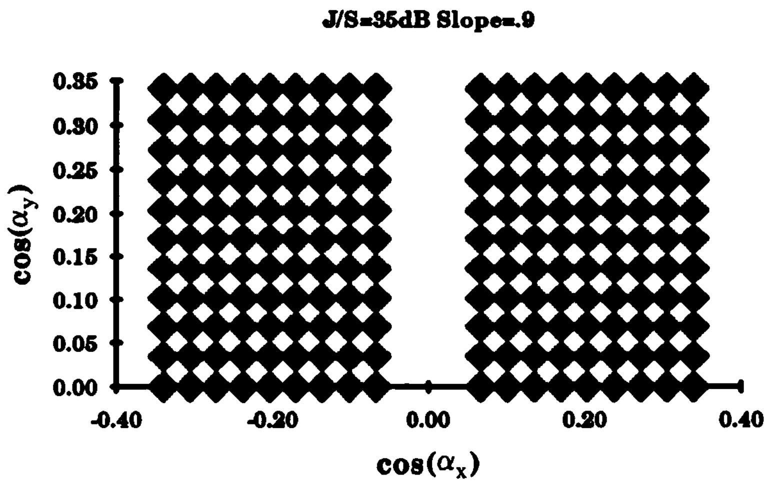

Figure 3.12. Scan area with a target located ±.25 degrees off beam center. J/S = 35 dB with the cross-polarization response slope equal to .9

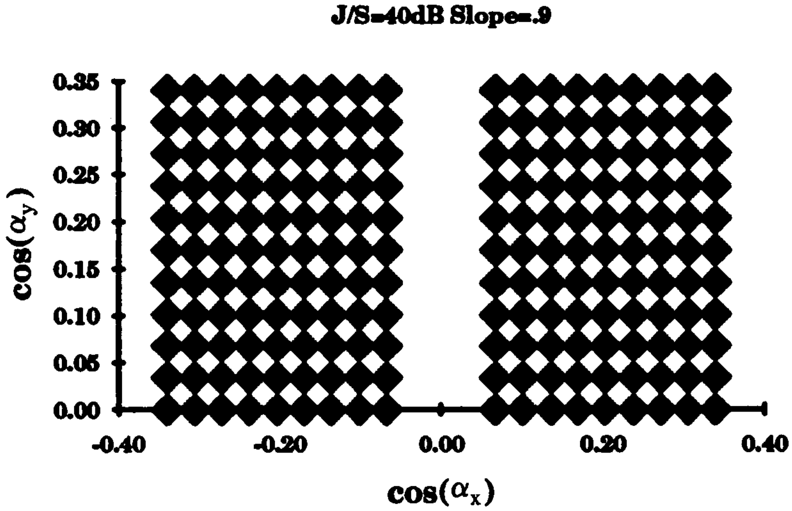

Figure 3.13. Scan area with a target located ±.25 degrees off beam center. J/S = 40 dB with the cross-polarization response slope equal to .9

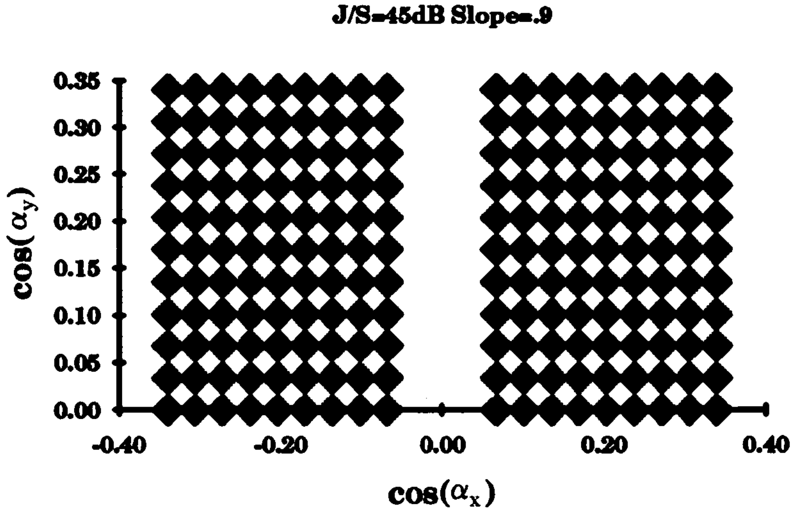

Figure 3.14. Scan area with a target located ±.25 degrees off beam center. J/S = 45 dB with the cross-polarization response slope equal to .9

This analysis shows that if the antennas co and cross-polarization responses are exactly the same, then naturally the antenna would be unaffected by cross-polarization jamming. However, small variations in the cross-polarization response from the co-polarization response causes a dramatic increase in the antenna's susceptibility.

Next, we examine phase shifters who's cross-polarization response is approximately opposite of the co-polarization response. Note, this case corresponds to the phase shifter response measured by Corey[12]. Figures 3.15 through 3.17 show the areas of susceptibility to cross-polarization jamming for a response slope of -.8, and various jammer powers. The antenna is relatively unaffected, with a slight increase in susceptibility with jammer power.

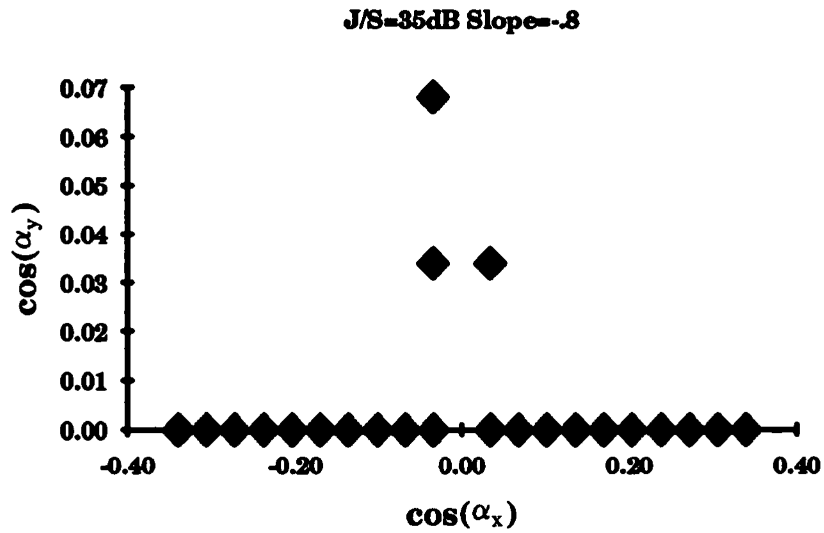

Figure 3.15. Scan area with targets located ±.25 degrees off beam center. J/S = 35 dB with the cross-polarization response slope equal to -.8

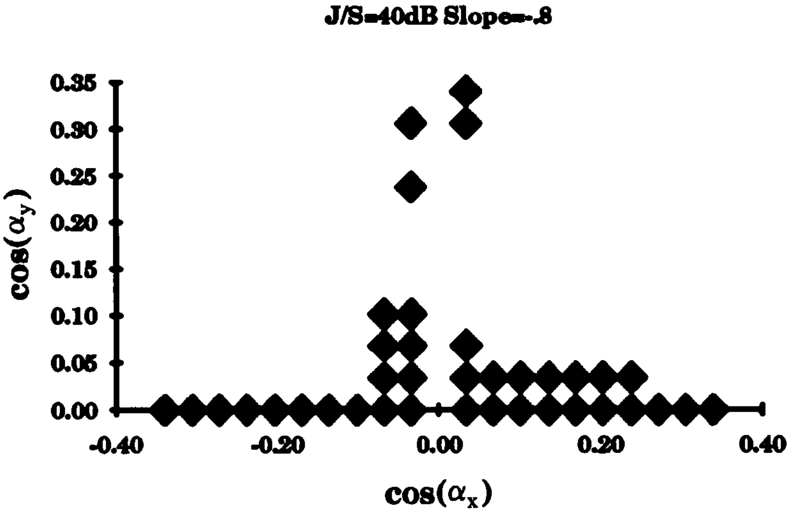

Figure 3.16. Scan area with a target located ±.25 degrees off beam center. J/S = 40 dB with the cross-polarization response slope equal to -.8

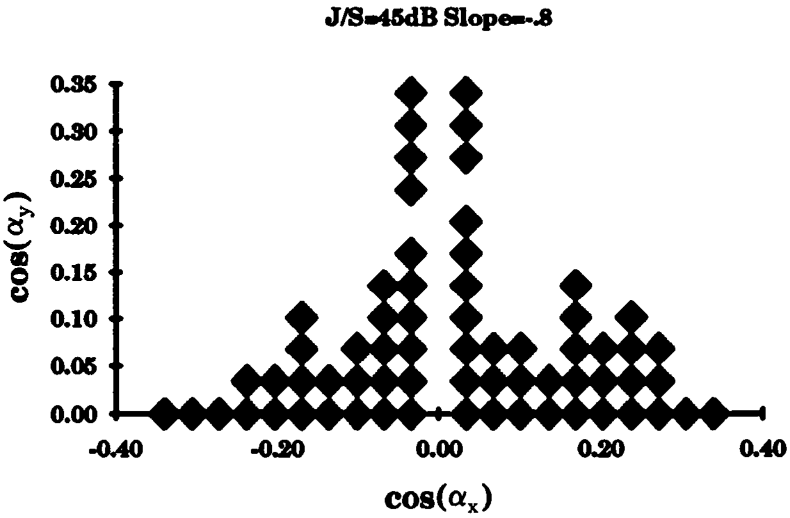

Figure 3.17. Scan area with a target located ±.25 degrees off beam center. J/S = 45 dB with the cross-polarization response slope equal to -.8

For a cross-polarization response slope of -.9, -.95, and -1, Figures 3.18 through 3.26 show the same trend (i.e., that the antenna is relatively unaffected over the scan area, with a slight increase in susceptibility with jammer power).

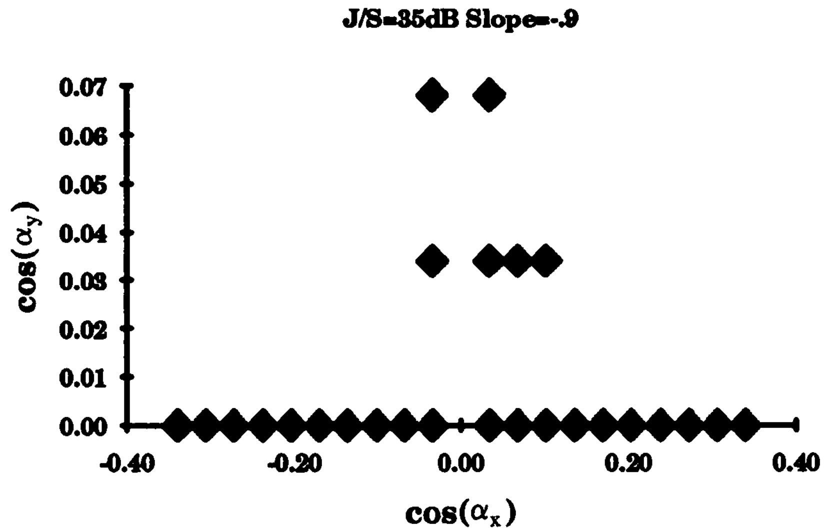

Figure 3.18. Scan area with a target located ±.25 degrees off beam center. J/S = 35 dB with the cross-polarization response slope equal to -.9

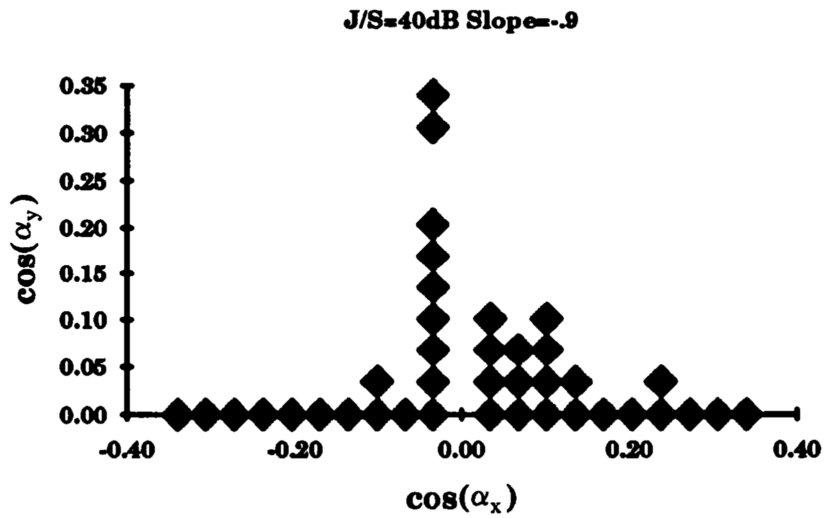

Figure 3.19. Scan area with a target located ±.25 degrees off beam center. J/S = 40 dB with the cross-polarization response slope equal to -.9

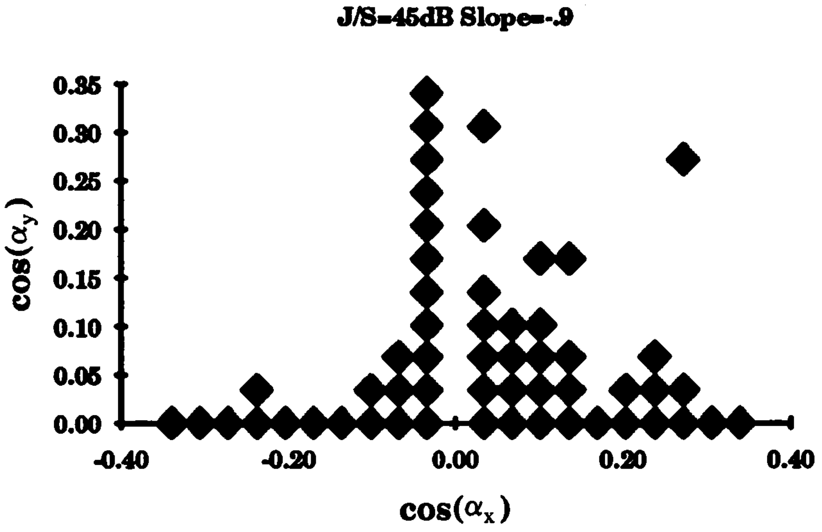

Figure 3.20. Scan area with targets located ±.25 degrees off beam center. J/S = 45 dB with the cross-polarization response slope equal to -.9

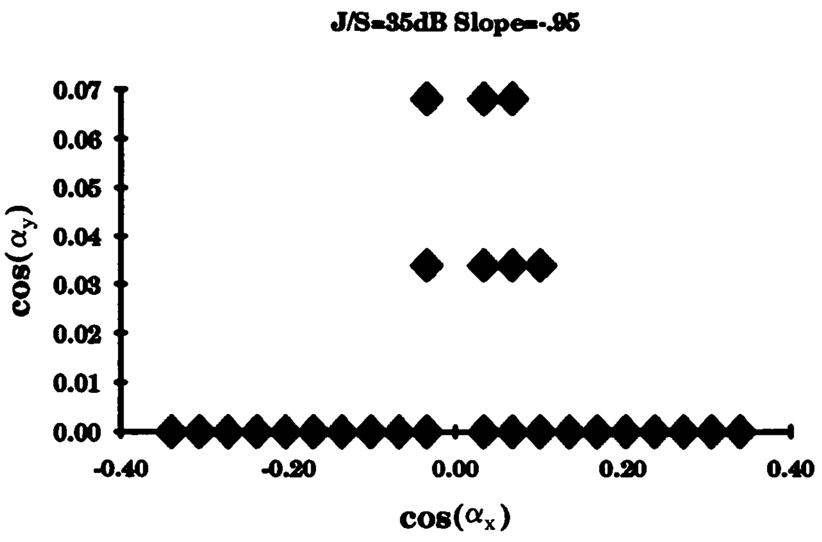

Figure 3.21. Scan area with a target located ±.25 degrees off beam center. J/S = 35 dB with the cross-polarization response slope equal to -.95

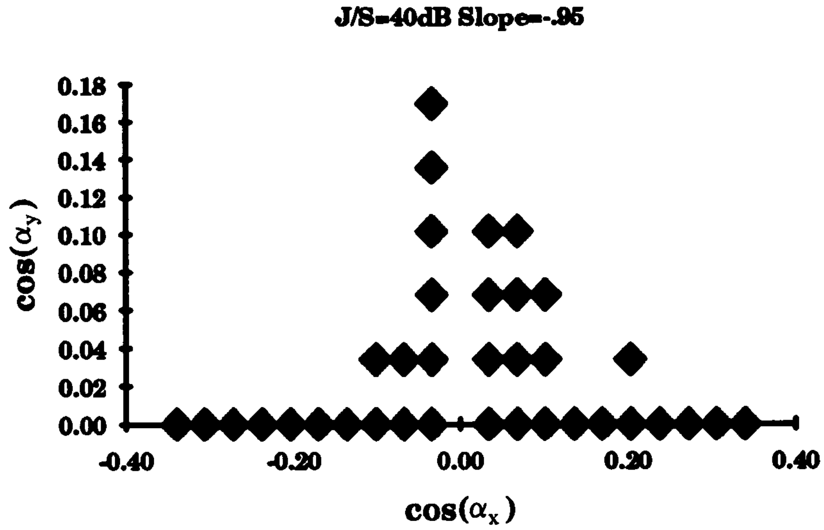

Figure 3.22. Scan area with a target located ±.25 degrees off beam center. J/S = 40 dB with the cross-polarization response slope equal to -.95

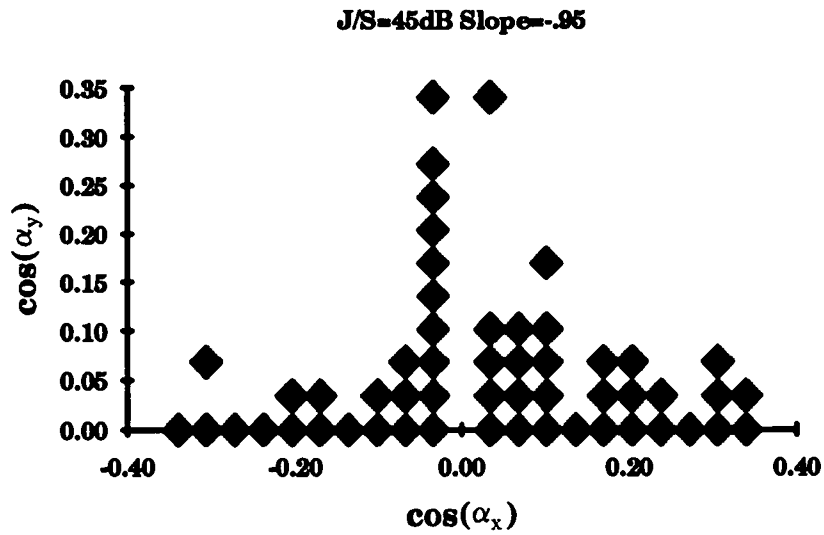

Figure 3.23. Scan area with a target located ±.25 degrees off beam center. J/S = 45 dB with the cross-polarization response slope equal to -.95

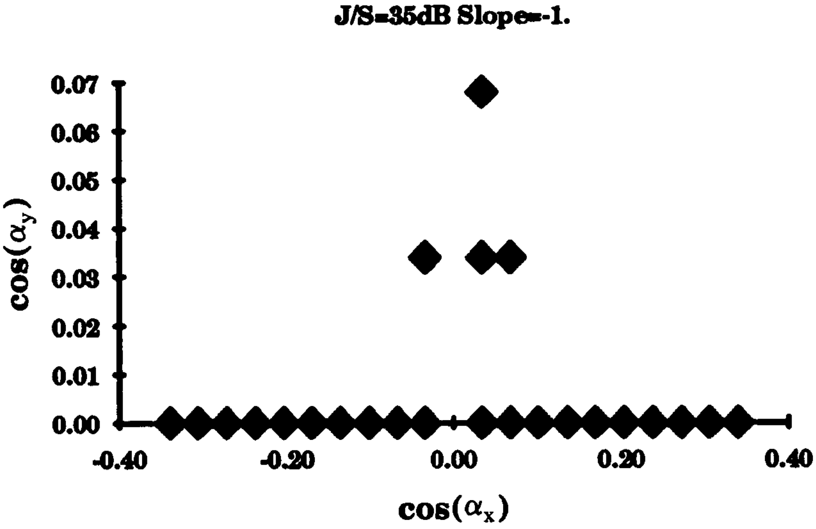

Figure 3.24. Scan area with a target located ±.25 degrees off beam center. J/S = 35 dB with the cross-polarization response slope equal to -1.

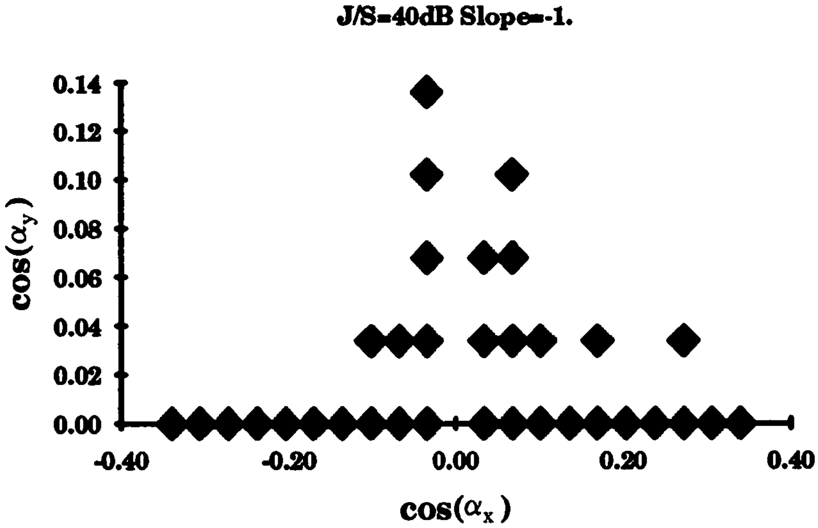

Figure 3.25. Scan area with targets located ±.25 degrees off beam center. J/S = 40 dB with the cross-polarization response slope equal to -1.

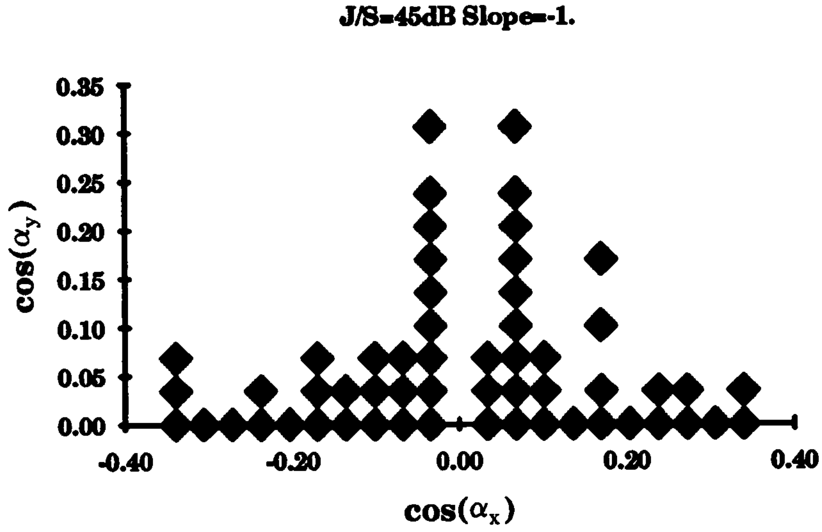

Figure 3.26. Scan area with a target located ±.25 degrees off beam center. J/S = 45 dB with the cross-polarization response slope equal to -1.

It now becomes evident that an antenna composed of phase shifters that have co and cross-polarization responses with opposite slopes are much less sensitive to cross-polarization jamming. Furthermore, the response is much less sensitive to small changes, or variations in the phase shifter design.

Table 3.1 gives a listing of the percentage of points in the scan area flagged as being susceptible to cross-polarization jamming for several cross-polarization response slopes. The test was performed for three jammer to signal (J/S) power ratios.

Table 3.1. Relative measure of susceptibility (δ) for various cross-polarization response slopes and J/S ratios.

Cross-Polarization Response Slope	J / S RATIO		
	35 dB	40 dB	45 dB
+1.00	0	0	0
+.97	57%	57%	57%
+.95	76%	76%	76%
+.90	86%	86%	86%
-.80	10%	16%	29%
-.90	11%	17%	24%
-.95	12%	16%	23%
-1.00	10%	15%	24%

Notice that for a cross-polarization response slope of +1, there were no points in the array's scan area that were evaluated as being susceptible to cross-polarization jamming, regardless of the J to S ratio. However, from table 3.1 it can be seen that as the response slope deviates from +1.0, the susceptibility to cross-polarization effects increases rapidly, even for small jammer powers. For the case where the response slope equals -1, the susceptibility was found to be low, and also relatively insensitive to variations around -1.

CHAPTER IV

CONCLUSION

The phased array antenna model for this study was a two dimensional phased array antenna model. Incorporated into the antenna model was the actual polarization characteristics of a circularly polarized Faraday rotator type phase shifter.

It was also observed that if the cross-polarization slope was +1.0, the array was virtually immune to cross-polarization jamming. In fact, it could be shown that the jammer would essentially become like a beacon. However, it was demonstrated that for relatively small perturbations away from +1.0, the susceptibility increased significantly. Also, for cross-polarization slopes of -1.0 the array seemed relatively insensitive to cross-polarization jamming.

From this analysis, one can conclude that a cross-polarization response of +1 is most desirable. However, small variations (which may result from inconsistencies in the manufacturing process, variations in operating temperature, etc.) may increase the antenna's susceptibility to cross-polarization jamming to an unacceptable level. On the other hand, for a cross-polarization response slope that varies around -1, and the antenna remains relatively immune to cross-polarization jamming. Therefore, a cross-polarization response slope of -1 would be the most practical design point.

LIST OF REFERENCES

LIST OF REFERENCES

1. Ogg, F. C. "Steerable Array Radars", IRE Trans., vol. MIL-5, pp. 80 - 94, April, 1961.

2. Allen, J. L. "The Theory of Antennas", MIT Lincoln Lab. Tech. Rept. 323, July, 1963.

3. Kraus, John D. Antennas, Second Edition. New York: McGraw-Hill Book Company, Inc., 1988.

4. Mailloux, Robert J. "Phased Array Theory and Technology", Proc. IEEE, vol. 70, no.3, March, 1982.

5. Skolnik, Merrill Radar Handbook. New York: McGraw-Hill Book Company, Inc., 1970.

6. Barton, David. Modern Radar System Analysis. Norwood, MA: Artech House, Inc., 1988.

7. Lax, Benjamin and Kenneth J. Button. Microwave Ferrites and Ferrimagnetics. New York: McGraw-Hill Book Company, Inc., 1962.

8. Hord, William E. and Boyd, Charles R. Jr. and Rosenbaum, Fred J. "Application of Reciprocal Latching Phase Shifter to Light Weight Electronic Scanned Phased Arrays", Prec. IEEE, vol 56, pp. 1931 - 1939, November, 1968.

9. Skolnik, Merrill. Radar Handbook, Second Edition. New York: McGraw Hill Publishing Co., 1990.

10. Proakis, John G and Manolakis, Dimitris G. Introduction To Digital Signal Processing. New York: Macmillan Publishing Company, 1988.

11. Sakiotis, N. G. and Chait, H. N. "Properties of Ferrites in Waveguides" Presented at the URSI-IRE meeting at the National Bureau of Standards, April 27-30, 1953.

12. Williams, S. P. and L. E. Corey. "Polarization Characteristics of Phased-Array Antennas Using Circularly Polarized Dual-Mode Ferrite Phase Shifters." Final Report from the Georgia Institute of Technology.

13. Van Brunt, Leroy B. Applied ECM Vol. 1,EW Engineering, Inc., 1978.

14. Shen, Liang Chi and Kong, Jin Av. Applied Electromagnetics. PWS Publishers, 1987

15. Gibson, Steven C. and Tae Jung Kim. Radar Cross Section Analysis by the Physical Theory of Diffraction Volume II - User's Manual. Northrup Corporation, Aircraft Division. March 1989.

16. Ruck, George T. Radar Cross Section Handbook Vol. 1. 1970.

17. Leonev, A. I. and K. I. Fomichev. Monopulse Radar. Norwood, MA: Artech House, Inc., 1986.

APPENDICES

APPENDIX A

Listed in table A.1, are several different ferrite materials and their associated polarization characteristics. The following Figures A.1. through A.7. are the calculated propagation constants for these materials in a 3% filled waveguide.

Table A.1. Ferrite characteristics. Adapted from Lax, Benjamin and Kenneth J. Button. Microwave Ferrites and Ferrimagnetics. New York: McGraw-Hill Book Company, Inc., 1962.

Manufacturer's type number	Saturation Magnetization	g_{eff}	ΔH	K_e	Dielectric Constant	Neel Temp T_n	Remarks
C3-P1	1450	2.5	300	9.5	.005	440	Ni(Al)
C6-P37	420	1.4	225	8.5	.003	155	Ni(Al)
C11-P16	3000	2.3	350	18.6	.006	575	Ni
TT-414	680	2.02	100	11.5	.0005	100	Mg,Mn(Al)
M-052	3150	2.27	140	12.0	.002	590	Ni(Co)
M-042	2390	2.45	1100	8.0	.002	590	Ni
TT-2-120	1800	2.55	1000	9.0	.0019	545	

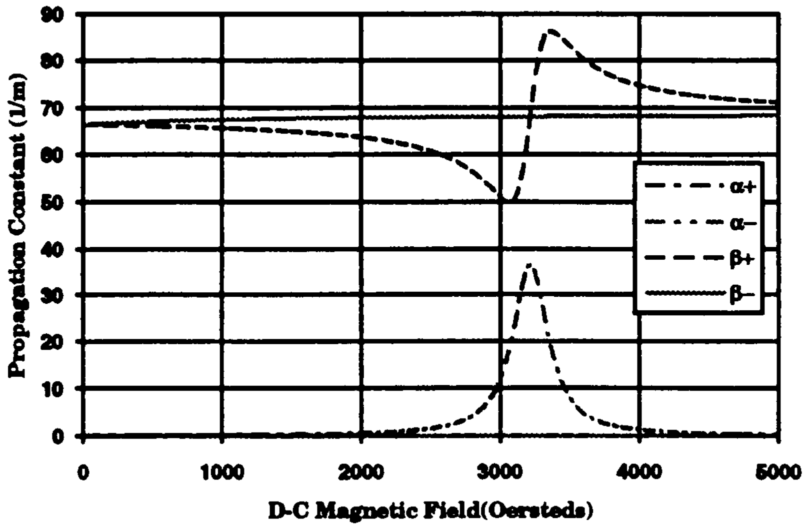

Figure A.1. Propagation constant for C3-P1 ferrite

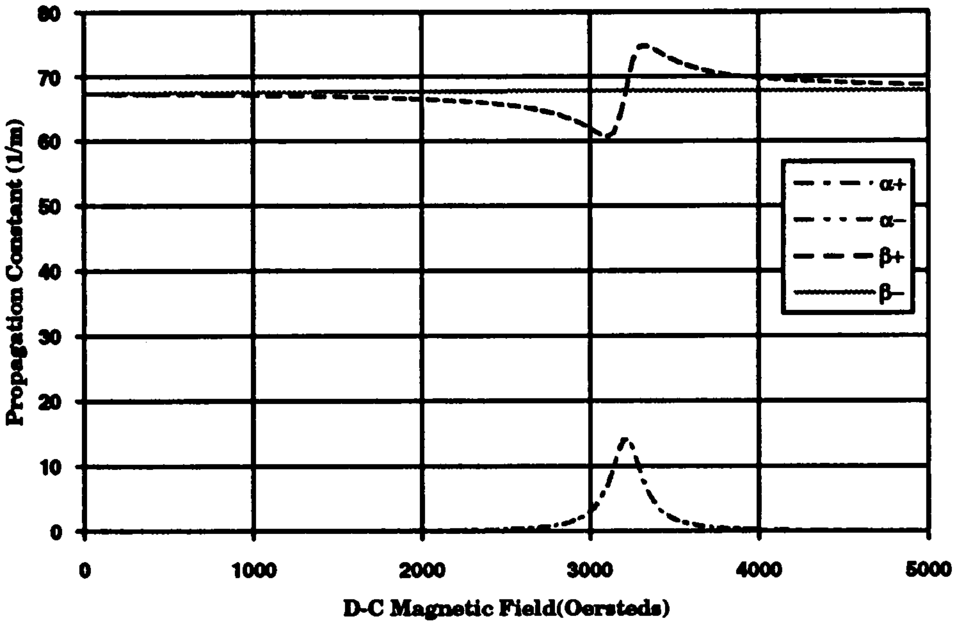

Figure A.2. Propagation constant for C6-P37 ferrite

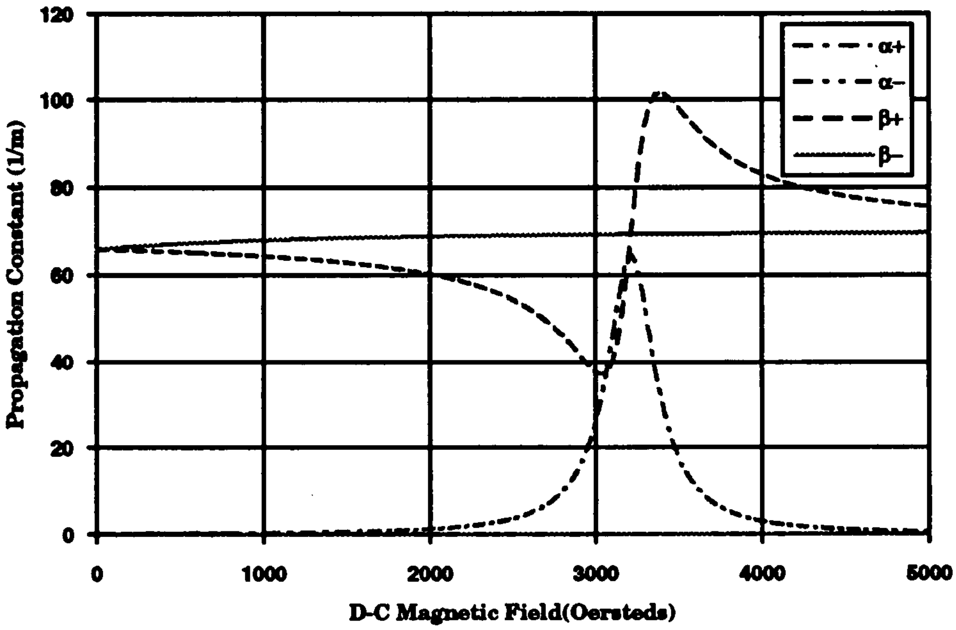

Figure A.3. Propagation constant for C11-P16 ferrite

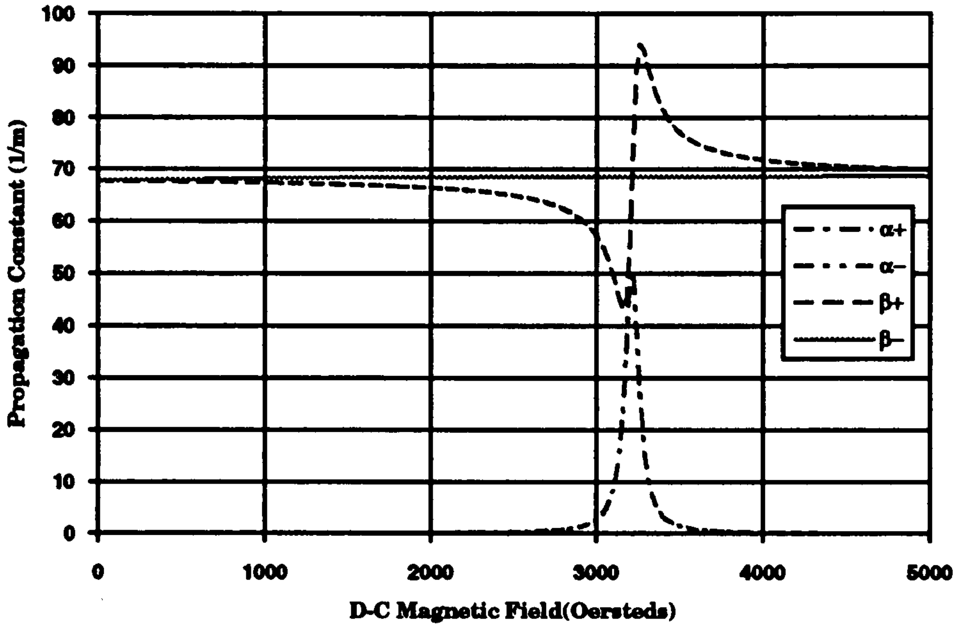

Figure A.4. Propagation constant for TT-414 ferrite

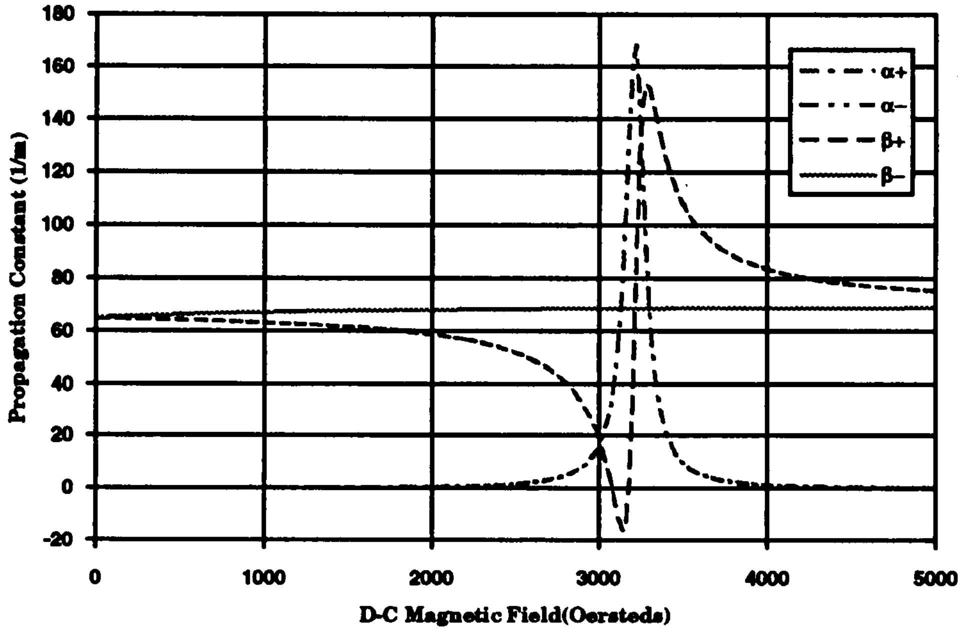

Figure A.5. Propagation constant for M-052 ferrite

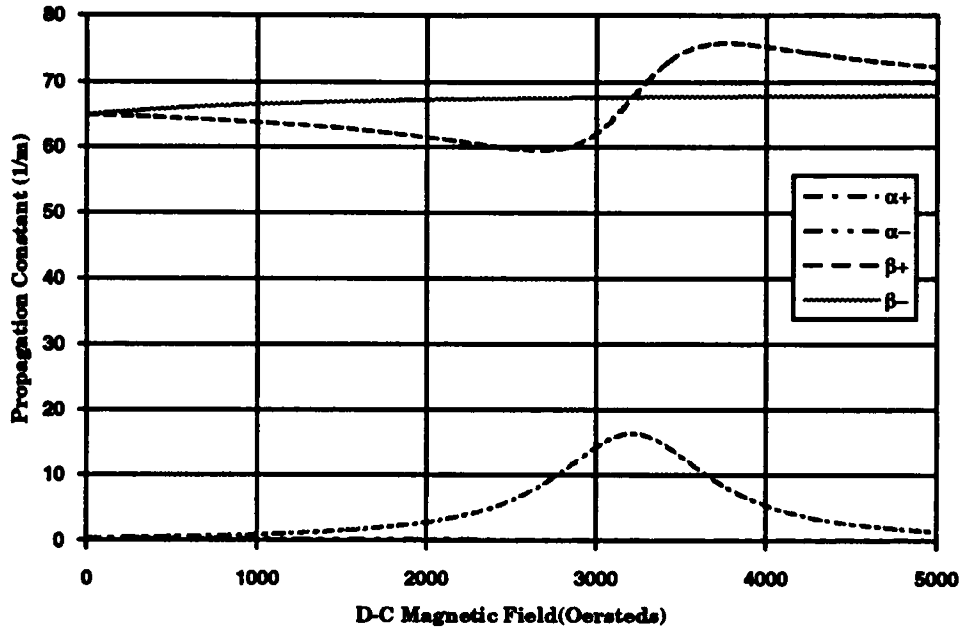

Figure A.6. Propagation constant for M-042 ferrite

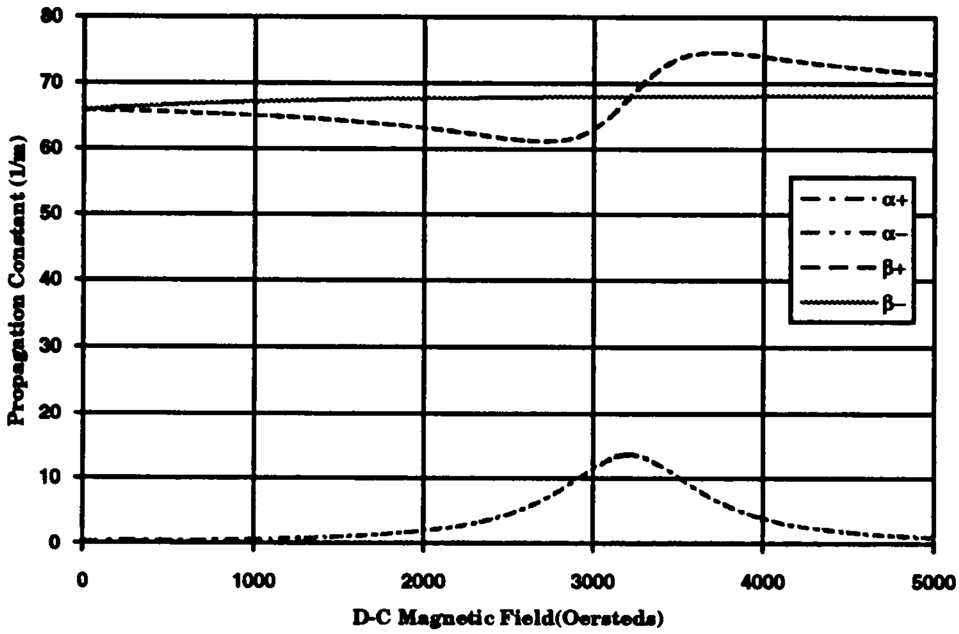

Figure A.7. Propagation constant for TT-2-120 ferrite

APPENDIX B

Appendix B contains listings of the antenna model computer code used in the preceeding paper.

```
c-
      subroutine driver(x,y,x_s,y_s,v1,v2,v3,v4)
      real pi,x,y,x_s,y_s,norm
      complex sum,d1,xsum,xd1,v1,v2,v3,v4

      pi = 3.14159d00

      norm = 1.

       call antena(x+x_s,y+y_s,x_s,y_s,sum,d1,xsum,xd1)

       v1 = sum/norm
       v2 = d1/norm
       v3 = xsum/norm
       v4 = xd1/norm

       return
       end
C---------------------------------------------
      subroutine antena(x,y,x_s,y_s,v1,v2,v3,v4)
      real x,y,pi,x_s,y_s
      complex b1,b2,b3,b4,sum,d1,v1,v2,v3,v4
      integer flg
      data b1,b2,b3,b4/0.0,0.0,0.0,0.0/

      pi = 3.14159d00
      squint = 0.00625
      flg = 1
      do 10 flg = 0,1

      call patt(flg,x+squint,y+squint,x_s,y_s,b1)

      call patt(flg,x+squint,y-squint,x_s,y_s,b2)

      call patt(flg,x-squint,y+squint,x_s,y_s,b3)

      call patt(flg,x-squint,y-squint,x_s,y_s,b4)

      sum = ((b1) + (b2) + (b3) + (b4))
      d1 = ((b3 + b4) - (b1 + b2))

          if (flg.eq.0) then
          v1 = sum
```

```
          v2 = d1
          else
          v3 = sum
          v4 = d1
          endif

10    continue

      return
      end
c-----------------------------------------------------
      subroutine patt(flg,x,y,x_s,y_s,e_fld)
      real x,y,x_s,y_s,phz(0:140,0:140),a,a0,a1,pi,re,im
      integer n_el,flg
      complex e_fld

      call phase(flg,x,y,x_s,y_s,phz)

      e_fld = (0.d00,0.d00)
      a1 = .5d00
      a0 = .5d00
      pi = 3.14159d00
      n_el = 70

      do 10 m = 0 ,n_el-1

      do 20 n = 0 , n_el-1

        a = 1.d00

        re = a*dcos(phz(m,n))
        im = a*dsin(phz(m,n))
        e_fld = e_fld + cmplx(re,im)

20    continue

10    continue

      return
      end
c-----------------------------------------------------
      subroutine phase(flg,x,y,x_s,y_s,phz)
      real x,y,x_s,y_s,pi,phz(0:140,0:140),t1,t2
      integer n,m,n_el,flg
```

```
      pi = 3.14159d00
      tx = pi*x
      txs = pi*x_s
      ty = pi*y
      tys = pi*y_s

      do 10 m = 0, n_el-1
c      m=(n_el-1)/2                    !
       do 20 n = 0, n_el-1

      quad = 2*pi*(sqrt(70**2 + (.5*n-((n_el-1)/4.))**2
     +          + (.5*m-((n_el-1)/4.))**2) - 70)

       t1 = m*tx + n*ty

c      chk = (m*txs+n*tys) + quad

       t2 = (m*txs + n*tys) + quad
       call bits(0,t2)
c        write(*,*)chk,t2
       t2 = t2 - quad
      if (flg.eq.1) call xphz(t2)
       phz(m,n) = t1 - t2

c        write(*,*)n,quad

20      continue
10     continue

c      stop
      return
      end

c--------------------------------------------------
      subroutine xphz(t2)
      real t2,slope,pi
      pi = 3.14159d00

      slope = -.8
      t2 = t2*slope + 2*pi
      call bits(0,t2)
      return
      end
```

```
c-------------------------------------------------
      subroutine bits(flg,phz)
      real qbits,pi,phz
      integer flg

      data qbits/.3927d00/
      data pi/3.1415926589d00/

     if (flg.eq.1) phz = mod(phz,2*pi)
     phz = idnint(phz/qbits+.5)*qbits

      return
      end
c-------------------------------------------------
```

VITA

William P. Gilchrist was born in Decatur, Alabama, on September 15, 1965. He is the son of Luke P. Gilchrist and the former Lynda J. Jenkins. He has one sister, Janet Elizabeth Keeling.

He completed his high school education at Albert P. Brewer High School at Florette, Alabama, in May 1983. In August, 1983 he began studies at Calhoun Community College. In August 1985, he transferred to the University of Alabama where he received his Bachelor of Science degree in Electrical Engineering in December 1988. Immediately following, he began work on a Master of Science degree in Engineering Science and Mechanics at the University of Tennessee Space Institute, Tullahoma, Tennessee.

Mr. Gilchrist was employed by the U. S. Army, PATRIOT Project Office in Huntsville, Alabama during the completion of this thesis.